

**FEATURES**

- ▶ Operates from 6 GHz to 18 GHz
- ▶ 25 dBm typical transmit state  $P_{SAT}$
- ▶ 22 dB typical transmit state small signal gain
- ▶ 18 dB typical receive state small signal gain
- ▶ 2.5 dB typical receive state noise figure
- ▶ Coupled power amplifier output for power detection

**APPLICATIONS**

- ▶ Phased array antenna
- ▶ Military radar
- ▶ Weather radar
- ▶ Communication links
- ▶ Electronic warfare

**GENERAL DESCRIPTION**

The ADTR1107 is a compact, 6 GHz to 18 GHz, front-end IC with an integrated power amplifier, low noise amplifier (LNA), and a reflective single-pole double-throw (SPDT) switch. These integrated features make the device ideal for phased array antenna and radar applications. The front-end IC offers 25 dBm of saturated output power ( $P_{SAT}$ ) and 22 dB small signal gain in transmit state, and

**FUNCTIONAL BLOCK DIAGRAM**

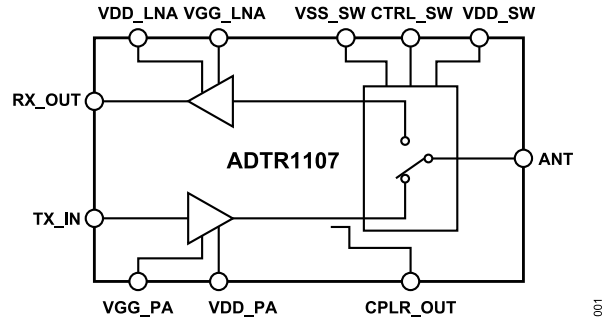


Figure 1.

18 dB small signal gain and 2.5 dB noise figure in receive state. The device has a directional coupler for power detection. The input/outputs (I/Os) are internally matched to 50  $\Omega$ . The ADTR1107 is supplied in a 5 mm  $\times$  5 mm, 24-terminal, land grid array (LGA) package.

**TABLE OF CONTENTS**

Features.....	1	Transmit State.....	9
Applications.....	1	Receive State.....	16
Functional Block Diagram.....	1	Theory of Operation.....	23
General Description.....	1	Applications Information.....	24
Specifications .....	3	Recommended Bias Sequencing.....	24
Absolute Maximum Ratings.....	6	Typical Application Circuit.....	25
Thermal Resistance.....	6	Interfacing the ADTR1107 to the ADAR1000 X	
ESD Caution.....	6	Band and KU Band Beamformer.....	26
Signal Path Truth Table.....	6	Outline Dimensions.....	27
Pin Configuration and Function Descriptions.....	7	Ordering Guide.....	27
Interface Schematics.....	7	Evaluation Boards.....	27
Typical Performance Characteristics.....	9		

**REVISION HISTORY****10/2022—Rev. A to Rev. B**

Changes to Applications Information Section.....	24
Changes to Figure 89.....	25

**4/2020—Rev. 0 to Rev. A**

Changes to VDD_LNA Parameter; Table 4.....	4
--	---

**1/2020—Revision 0: Initial Version**

## SPECIFICATIONS

Transmit state, VDD\_PA = 5 V, I<sub>DQ\_PA</sub> = 220 mA, VDD\_SW = 3.3 V, VSS\_SW = -3.3 V, CTRL\_SW = 0 V, receive state off (VDD\_LNA = 0 V, VGG\_LNA = 0 V), T<sub>A</sub> = 25°C, unless otherwise noted.

Table 1.

Parameter	Symbol	Min	Typ	Max	Unit	Test Conditions/Comments
OVERALL FUNCTION						
Frequency Range		6		14	GHz	
TRANSMIT STATE						
Small Signal Gain		19.5	21.5		dB	TX_IN to ANT
Gain Flatness			±0.8		dB	
Input Return Loss			13		dB	TX_IN to ANT
Output Return Loss			15		dB	TX_IN to ANT
Output 1 dB Compression (OP1dB)		21	23		dBm	TX_IN to ANT
Saturated Output Power (P <sub>SAT</sub> )			25		dBm	
Output Third-Order Intercept (OIP3)			31		dBm	TX_IN to ANT output power (P <sub>OUT</sub> ) per tone = 8 dBm
Noise Figure			9		dB	TX_IN to ANT
Coupling Factor			23.5		dB	Coupling factor = ANT P <sub>OUT</sub> - CPLR_OUT P <sub>OUT</sub>
Isolation						
TX_IN to RX_OUT			40		dB	Receive state off
ANT to RX_OUT			64		dB	Receive state off
RF Settling Time						
0.1 dB			17		ns	50% CTRL_SW to 0.1 dB of final RF output
0.05 dB			22		ns	50% CTRL_SW to 0.05 dB of final RF output
Switching Speed						
Rise and Fall Time	t <sub>RISE</sub> , t <sub>FALL</sub>		2		ns	10% to 90% of RF output
Turn On and Turn Off Time	t <sub>ON</sub> , t <sub>OFF</sub>		10		ns	50% CTRL_SW to 90% of RF output
VDD_PA		3.3	5.0	5.5	V	
Quiescent Current (I <sub>DQ_PA</sub> )			220		mA	Adjust VGG_PA voltage between -1.75 V and -0.25 V to achieve the desired I <sub>DQ_PA</sub>

Transmit state, VDD\_PA = 5 V, I<sub>DQ\_PA</sub> = 220 mA, VDD\_SW = 3.3 V, VSS\_SW = -3.3 V, CTRL\_SW = 0 V, receive state off, T<sub>A</sub> = 25°C, unless otherwise noted.

Table 2.

Parameter	Symbol	Min	Typ	Max	Unit	Test Conditions/Comments
OVERALL FUNCTION						
Frequency Range		14		18	GHz	
TRANSMIT STATE						
Small Signal Gain		20	22		dB	TX_IN to ANT
Gain Flatness			±0.6		dB	
Input Return Loss			12		dB	TX_IN to ANT
Output Return Loss			11		dB	TX_IN to ANT
OP1dB		19	21.5		dBm	TX_IN to ANT
P <sub>SAT</sub>			24		dBm	TX_IN to ANT
OIP3			31.5		dBm	TX_IN to ANT P <sub>OUT</sub> per tone = 8 dBm
Noise Figure			6.5		dB	TX_IN to ANT
Coupling Factor			18		dB	Coupling factor = ANT P <sub>OUT</sub> - CPLR_OUT P <sub>OUT</sub>
Isolation						
TX_IN to RX_OUT			39		dB	Receive state off
ANT to RX_OUT			64		dB	Receive state off
RF Settling Time						

## SPECIFICATIONS

Table 2.

Parameter	Symbol	Min	Typ	Max	Unit	Test Conditions/Comments
0.1 dB			17		ns	50% CTRL_SW to 0.1 dB of final RF output
0.05 dB			22		ns	50% CTRL_SW to 0.05 dB of final RF output
Switching Speed						
Rise and Fall Time	$t_{RISE}, t_{FALL}$		2		ns	10% to 90% of RF output
Turn On and Turn Off Time	$t_{ON}, t_{OFF}$		10		ns	50% CTRL_SW to 90% of RF output
VDD_PA		3.3	5.0	5.5	V	
I <sub>DQ_PA</sub>			220		mA	Adjust VGG_PA voltage between -1.75 V and -0.25 V to achieve the desired I <sub>DQ_PA</sub>

Receive state, self biased, VDD\_LNA = 3.3 V, VGG\_LNA = 0 V, VDD\_SW = 3.3 V, VSS\_SW = -3.3 V, CTRL\_SW = 3.3 V, transmit state off (VDD\_PA = 0 V, VGG\_PA = -1.75 V), T<sub>A</sub> = 25°C, unless otherwise noted.

Table 3.

Parameter	Symbol	Min	Typ	Max	Unit	Test Conditions/Comments
OVERALL FUNCTION						
Frequency Range		6		14	GHz	
RECEIVE STATE						
Small Signal Gain		15.5	17.5		dB	ANT to RX_OUT
Gain Flatness			±0.6		dB	
Input Return Loss			13		dB	ANT to RX_OUT
Output Return Loss			14		dB	ANT to RX_OUT
OP1dB		12	14		dBm	ANT to RX_OUT
P <sub>SAT</sub>			16		dBm	
OIP3			26		dBm	ANT to RX_OUT P <sub>OUT</sub> per tone = 0 dBm
Noise Figure			2.5		dB	ANT to RX_OUT
Isolation						
ANT to TX_IN			32		dB	Transmit state off
RX_OUT to TX_IN			48		dB	Transmit state off
RF Settling Time						
0.1 dB			17		ns	50% CTRL_SW to 0.1 dB of final RF output
0.05 dB			22		ns	50% CTRL_SW to 0.05 dB of final RF output
Switching Speed						
Rise and Fall Time	$t_{RISE}, t_{FALL}$		2		ns	10% to 90% of RF output
Turn On and Turn Off Time	$t_{ON}, t_{OFF}$		10		ns	50% CTRL_SW to 90% of RF output
VDD_LNA		2.0	3.3	3.6	V	
I <sub>DQ_LNA</sub>			80		mA	Self biased

Receive state, self biased, VDD\_LNA = 3.3 V, VGG\_LNA = 0 V, VDD\_SW = 3.3 V, VSS\_SW = -3.3 V, CTRL\_SW = 3.3 V, transmit state off, T<sub>A</sub> = 25°C, unless otherwise noted.

Table 4.

Parameter	Symbol	Min	Typ	Max	Unit	Test Conditions/Comments
OVERALL FUNCTION						
Frequency Range		14		18	GHz	
RECEIVE STATE						
Small Signal Gain		16	18		dB	ANT to RX_OUT
Gain Flatness			±0.9		dB	
Input Return Loss			13		dB	ANT to RX_OUT
Output Return Loss			18		dB	ANT to RX_OUT

## SPECIFICATIONS

Table 4.

Parameter	Symbol	Min	Typ	Max	Unit	Test Conditions/Comments
OP1dB		12	14		dBm	ANT to RX_OUT
P <sub>SAT</sub>			16.5		dBm	ANT to RX_OUT
OIP3			25.5		dBm	ANT to RX_OUT P <sub>OUT</sub> per tone = 0 dBm
Noise Figure			3		dB	ANT to RX_OUT
Isolation						
ANT to TX_IN			26		dB	Transmit state off
RX_OUT to TX_IN			46		dB	Transmit state off
RF Settling Time						
0.1 dB			17		ns	50% CTRL_SW to 0.1 dB of final RF output
0.05 dB			22		ns	50% CTRL_SW to 0.05 dB of final RF output
Switching Speed						
Rise and Fall Time	t <sub>RISE</sub> , t <sub>FALL</sub>		2		ns	10% to 90% of RF output
Turn On and Turn Off Time	t <sub>ON</sub> , t <sub>OFF</sub>		10		ns	50% CTRL_SW to 90% of RF output
VDD_LNA		2.0	3.3	3.6	V	
I <sub>DQ</sub> _LNA			80		mA	Self biased

SPDT switch bias at VDD\_SW = 3.3 V, VSS\_SW = -3.3 V.

Table 5.

Parameter	Symbol	Min	Typ	Max	Unit	Test Conditions/Comments
SUPPLY CURRENT						VDD_SW and VSS_SW
Positive	IDD_SW		14		μA	
Negative	ISS_SW		120		μA	
DIGITAL CONTROL INPUTS						CTRL_SW
Voltage						
Low		0		0.8	V	
High		1.2		3.3	V	
Current (Low and High)			<1		μA	

## ABSOLUTE MAXIMUM RATINGS

**Table 6.**

Parameter	Rating
Transmit State (PA On), Receive State Off	
VDD_PA	5.5 V
VGG_PA	-2 V to +0 V
Continuous Wave (CW) RF Input Power (RFIN) at TX_IN	20 dBm
Continuous Power Dissipation ( $P_{DISS}$ ) ( $T_A = 85^\circ\text{C}$ , Derate 18.98 mW/ $^\circ\text{C}$ Above $85^\circ\text{C}$ )	1.71 W
Receive State (LNA On), Transmit State Off	
VDD_LNA	4 V
VGG_LNA	-2 V to +0.2 V
CW RFIN at ANT	20 dBm
$P_{DISS}$ ( $T_A = 85^\circ\text{C}$ , Derate 5.04 mW/ $^\circ\text{C}$ Above $85^\circ\text{C}$ )	0.453 W
Transmit and Receive States	
Output Load Voltage Standing Wave Ratio (VSWR)	7:1
VDD_SW Range	-0.3 V to +3.6 V
VSS_SW Range	-3.6 V to +0.3 V
VDD_CTRL Range	-0.3 V to VDD + 0.3 V
Channel Temperature	175 $^\circ\text{C}$
Maximum Peak Reflow Temperature (Moisture Sensitivity Level 3, MSL3) <sup>1</sup>	260 $^\circ\text{C}$
Storage Temperature Range	-40 $^\circ\text{C}$ to +125 $^\circ\text{C}$
Operating Temperature Range	-40 $^\circ\text{C}$ to +85 $^\circ\text{C}$
ESD Sensitivity (Human Body Model)	Class 1B (Passed $\pm 500$ V)

<sup>1</sup> See the [Ordering Guide](#) section for more information.

Stresses at or above those listed under Absolute Maximum Ratings may cause permanent damage to the product. This is a stress

## SIGNAL PATH TRUTH TABLE

**Table 8. Signal Path Truth Table**

State	CTRL_SW	RF Signal Path
Transmit	Low	TX_IN to ANT
Receive	High	ANT to RX_OUT

rating only; functional operation of the product at these or any other conditions above those indicated in the operational section of this specification is not implied. Operation beyond the maximum operating conditions for extended periods may affect product reliability.

## THERMAL RESISTANCE

Thermal performance is directly linked to printed circuit board (PCB) design and operating environment. Careful attention to PCB thermal design is required.

$\theta_{JC}$  is the thermal resistance from the operating portion of the device to the outside surface of the package (case) closest to the device mounting area.

**Table 7. Thermal Resistance**

Package Type <sup>1</sup>	$\theta_{JC}$ Transmit State	$\theta_{JC}$ Receive State	Unit
CC-24-8	52.7	198.4	$^\circ\text{C}/\text{W}$

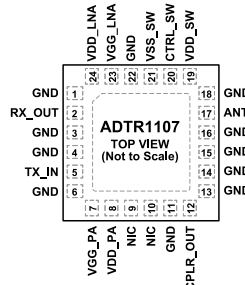
<sup>1</sup> Thermal impedance simulated values are based on a JEDEC 2S2P thermal test board with 36 thermal vias. Refer to the JEDEC standard JESD51 for additional information.

## ESD CAUTION



**ESD (electrostatic discharge) sensitive device.** Charged devices and circuit boards can discharge without detection. Although this product features patented or proprietary protection circuitry, damage may occur on devices subjected to high energy ESD. Therefore, proper ESD precautions should be taken to avoid performance degradation or loss of functionality.

PIN CONFIGURATION AND FUNCTION DESCRIPTIONS



NOTES  
 1. NIC = NO INTERNAL CONNECTION. SOLDER THESE PINS TO A LOW IMPEDANCE GROUND PLANE.  
 2. EXPOSED PAD, MUST BE CONNECTED TO RF/DC GROUND.

Figure 2. Pin Configuration

Table 9. Pin Function Descriptions

Pin No.	Mnemonic	Description
1, 3, 4, 6, 11, 13 to 16, 18, 22	GND	Ground. Solder these pins to a low impedance ground plane.
2	RX_OUT	Receive Path Output. This pin is dc-coupled to ground and ac matched to 50 Ω.
5	TX_IN	Transmit Path Input. This pin is dc-coupled to ground and ac matched to 50 Ω.
7	VGG_PA	Power Amplifier Gate Bias. This pin is used to set the desired quiescent current of the amplifier.
8	VDD_PA	Power Amplifier Drain Bias Voltage.
9, 10	NIC	No Internal Connection. Solder these pins to a low impedance ground plane.
12	CPLR_OUT	Transmit Path Coupled Port. This port is used in connection with a detector to monitor transmitted power.
17	ANT	RF Common Port. This pin is dc-coupled to 0 V and ac matched to 50 Ω.
19	VDD_SW	SPDT Switch Positive Bias Voltage.
20	CTRL_SW	Switch Digital Control. This pin controls the state of the SPDT switch.
21	VSS_SW	SPDT Switch Negative Bias Voltage.
23	VGG_LNA	LNA Gate Voltage Bias. This pin is used to set the desired quiescent current of the LNA. If this pin is supplied with 0 V or is connected to ground, the LNA runs in self bias mode at a typical current of 80 mA.
24	VDD_LNA	LNA Drain Voltage Bias.
	EPAD	Exposed Pad. Must be connected to RF/dc ground.

INTERFACE SCHEMATICS



Figure 3. GND Interface Schematic

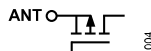


Figure 4. ANT Interface Schematic

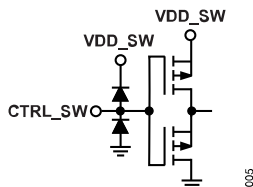


Figure 5. CTRL\_SW and VDD\_SW Interface Schematic

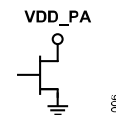


Figure 6. VDD\_PA Interface Schematic

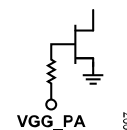


Figure 7. VGG\_PA Interface Schematic

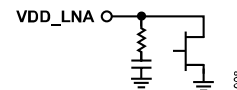


Figure 8. VDD\_LNA Interface Schematic

## PIN CONFIGURATION AND FUNCTION DESCRIPTIONS

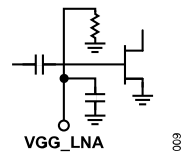


Figure 9. VGG\_LNA Interface Schematic

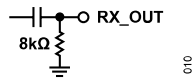


Figure 10. RX\_OUT Interface Schematic

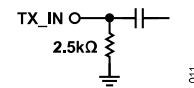


Figure 11. TX\_IN Interface Schematic



TYPICAL PERFORMANCE CHARACTERISTICS

TRANSMIT STATE

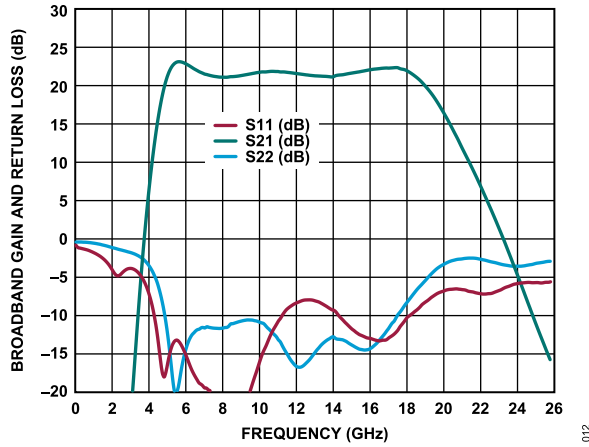


Figure 12. Broadband Gain and Return Loss vs. Frequency, 10 MHz to 26 GHz, Transmit State, Path = TX\_IN to ANT, VDD\_PA = 5 V, IDQ\_PA = 220 mA, Receive State Off

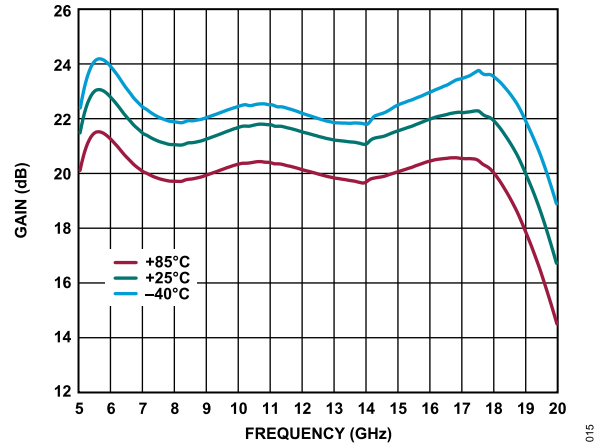


Figure 15. Gain vs. Frequency for Various Temperatures, Transmit State, Path = TX\_IN to ANT, VDD\_PA = 5 V, IDQ\_PA = 220 mA, Receive State Off

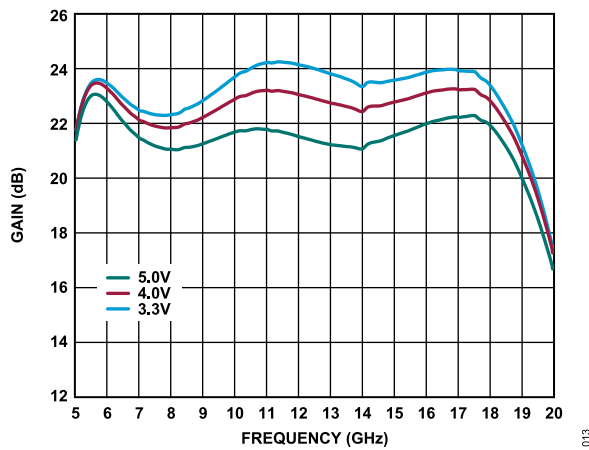


Figure 13. Gain vs. Frequency for Various VDD\_PA, Transmit State, Path = TX\_IN to ANT, IDQ\_PA = 220 mA, Receive State Off

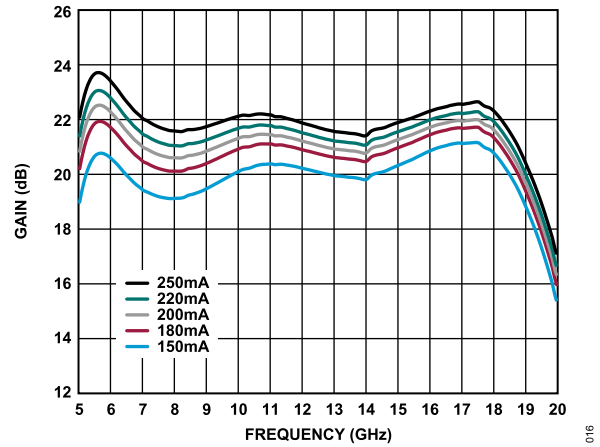


Figure 16. Gain vs. Frequency for Various IDQ\_PA, Transmit State, Path = TX\_IN to ANT, VDD\_PA = 5 V, Receive State Off

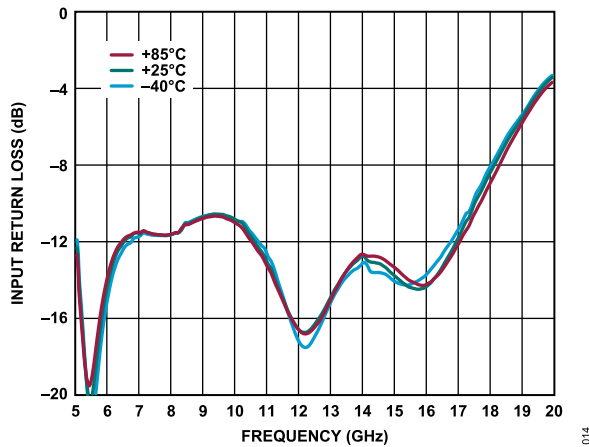


Figure 14. Input Return Loss vs. Frequency for Various Temperatures, Transmit State, Path = TX\_IN to ANT, VDD\_PA = 5 V, IDQ\_PA = 220 mA, Receive State Off

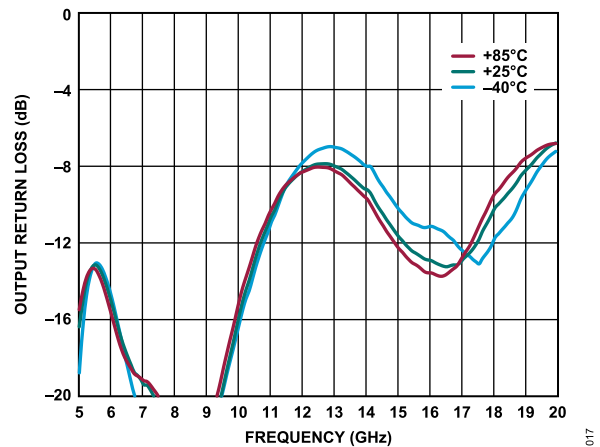


Figure 17. Output Return Loss vs. Frequency for Various Temperatures, Transmit State, Path = TX\_IN to ANT, VDD\_PA = 5 V, IDQ\_PA = 220 mA, Receive State Off

TYPICAL PERFORMANCE CHARACTERISTICS

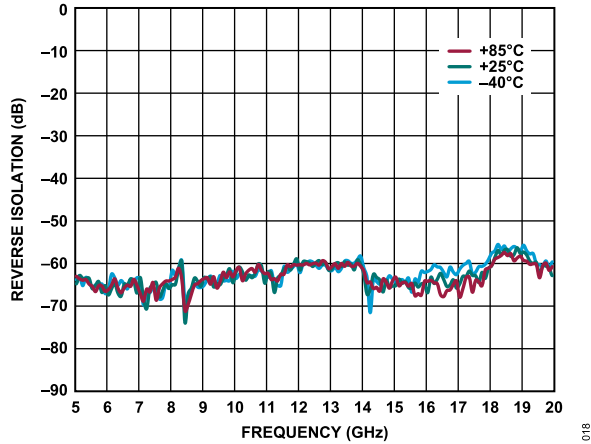


Figure 18. Reverse Isolation vs. Frequency for Various Temperatures, Transmit State, Path = TX\_IN to ANT, VDD\_PA = 5 V, I<sub>DQ\_PA</sub> = 220 mA, Receive State Off

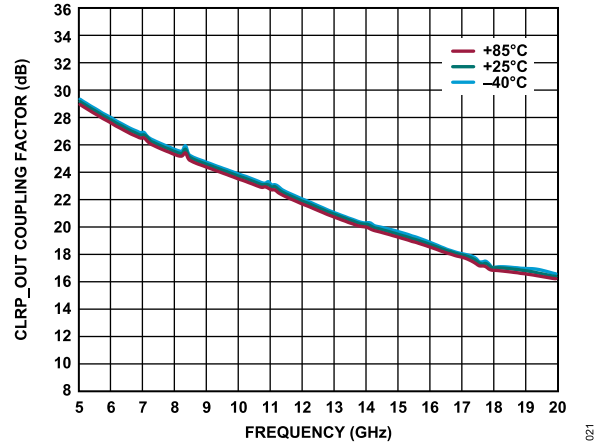


Figure 21. CLPR\_OUT Coupling Factor vs. Frequency for Various Temperatures, Transmit State, Coupling Factor = ANT P<sub>OUT</sub> - CPLR\_OUT P<sub>OUT</sub>, VDD\_PA = 5 V, I<sub>DQ\_PA</sub> = 220 mA, Receive State Off

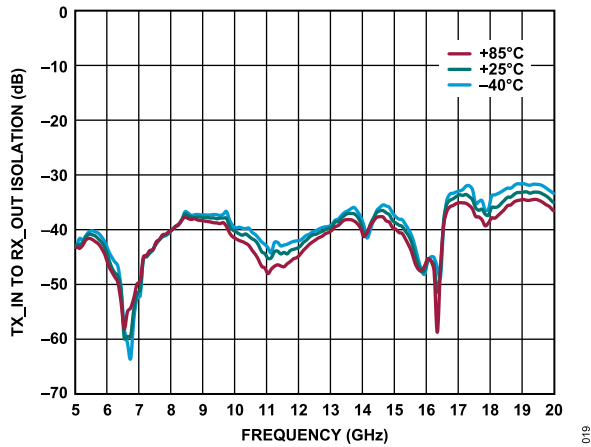


Figure 19. TX\_IN to RX\_OUT Isolation vs. Frequency for Various Temperatures, Transmit State, VDD\_PA = 5 V, I<sub>DQ\_PA</sub> = 220 mA, Receive State Off

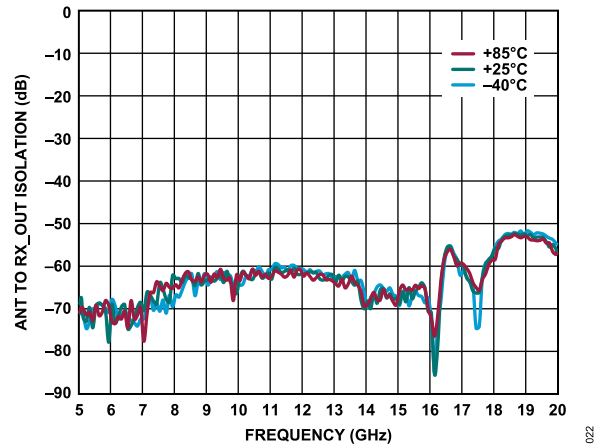


Figure 22. ANT to RX\_OUT Isolation vs. Frequency for Various Temperatures, Transmit State, VDD\_PA = 5 V, I<sub>DQ\_PA</sub> = 220 mA, Receive State Off

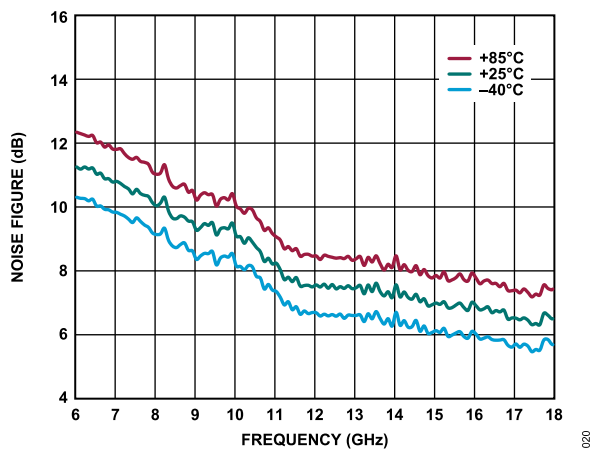


Figure 20. Noise Figure vs. Frequency for Various Temperatures, Transmit State, Path = TX\_IN to ANT, VDD\_PA = 5 V, I<sub>DQ\_PA</sub> = 220 mA, Receive State Off

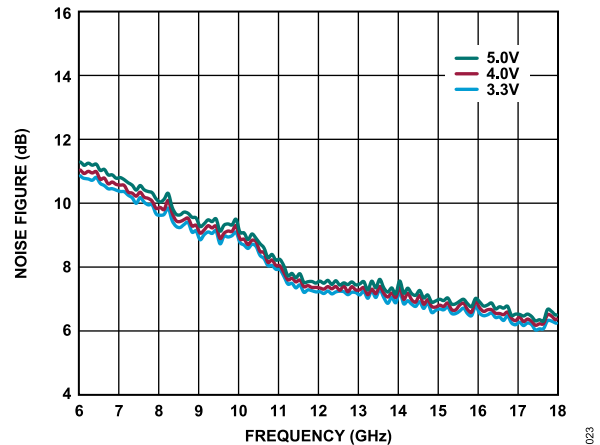


Figure 23. Noise Figure vs. Frequency for Various VDD\_PA, Transmit State, Path = TX\_IN to ANT, I<sub>DQ\_PA</sub> = 220 mA, Receive State Off

TYPICAL PERFORMANCE CHARACTERISTICS

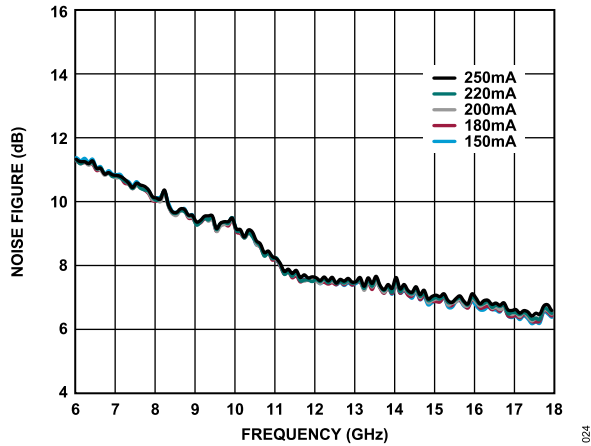


Figure 24. Noise Figure vs. Frequency for Various  $I_{DQ\_PA}$ , Transmit State, Path = TX\_IN to ANT, VDD\_PA = 5 V, Receive State Off

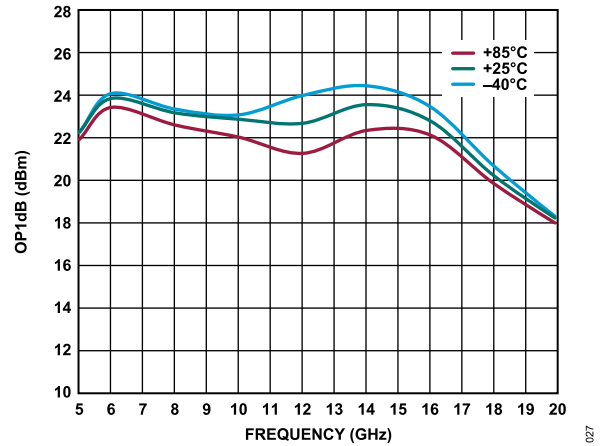


Figure 27. OP1dB vs. Frequency for Various Temperatures, Transmit State, Path = TX\_IN to ANT, VDD\_PA = 5 V,  $I_{DQ\_PA}$  = 220 mA, Receive State Off

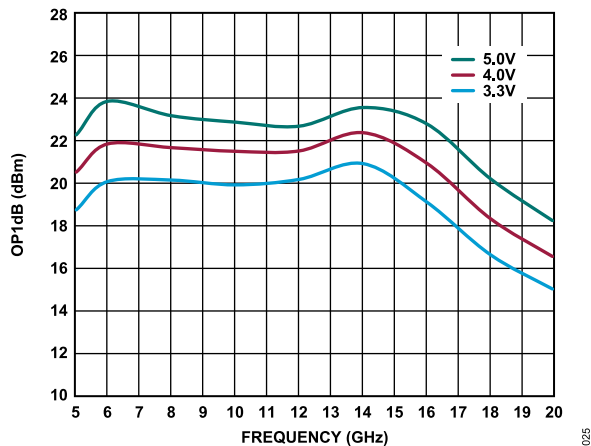


Figure 25. OP1dB vs. Frequency for Various VDD\_PA, Transmit State, Path = TX\_IN to ANT,  $I_{DQ\_PA}$  = 220 mA, Receive State Off

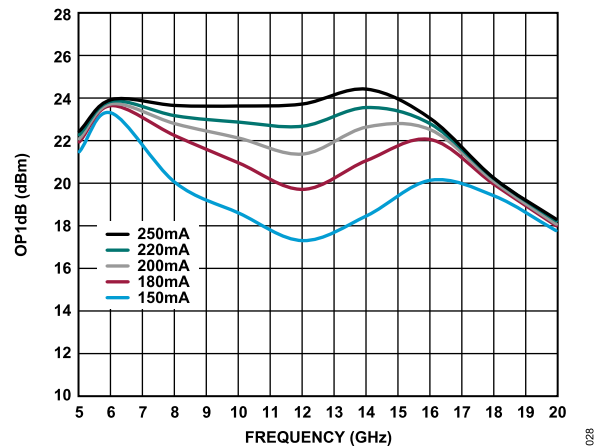


Figure 28. OP1dB vs. Frequency for Various  $I_{DQ\_PA}$ , Transmit State, Path = TX\_IN to ANT, VDD\_PA = 5 V, Receive State Off

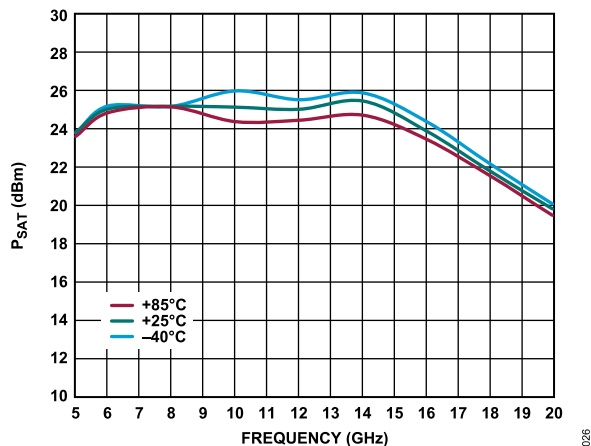


Figure 26.  $P_{SAT}$  vs. Frequency for Various Temperatures, Transmit State, Path = TX\_IN to ANT, VDD\_PA = 5 V,  $I_{DQ\_PA}$  = 220 mA, Receive State Off

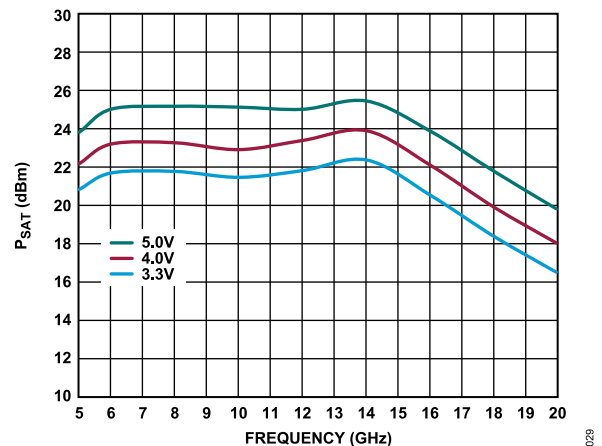


Figure 29.  $P_{SAT}$  vs. Frequency for Various VDD\_PA, Transmit State, Path = TX\_IN to ANT,  $I_{DQ\_PA}$  = 220 mA, Receive State Off

TYPICAL PERFORMANCE CHARACTERISTICS

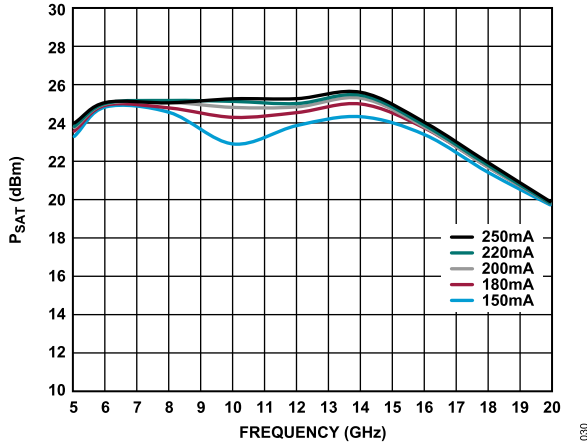


Figure 30.  $P_{SAT}$  vs. Frequency for Various  $I_{DQ\_PA}$ , Transmit State, Path = TX\_IN to ANT,  $V_{DD\_PA} = 5\text{ V}$ , Receive State Off

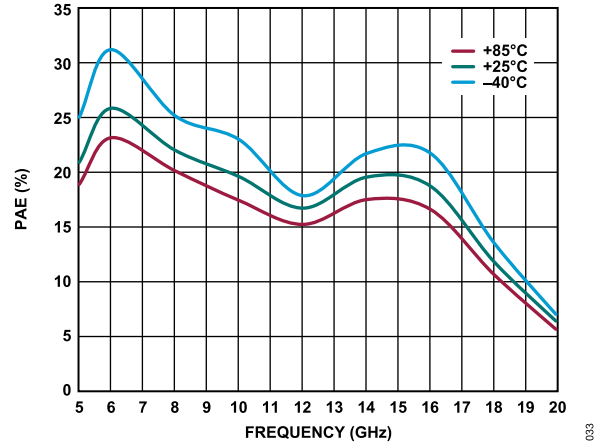


Figure 33. PAE vs. Frequency for Various Temperatures, Transmit State, Path = TX\_IN to ANT,  $V_{DD\_PA} = 5\text{ V}$ ,  $I_{DQ\_PA} = 220\text{ mA}$ , Receive State Off, PAE Measured at  $P_{SAT}$

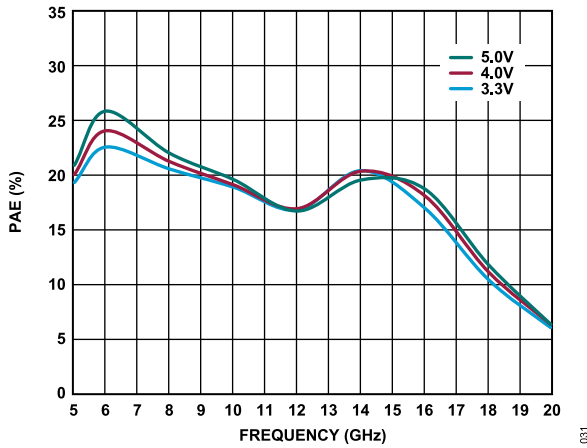


Figure 31. Power Added Efficiency (PAE) vs. Frequency for Various  $V_{DD\_PA}$ , Transmit State, Path = TX\_IN to ANT,  $I_{DQ\_PA} = 220\text{ mA}$ , Receive State Off, PAE Measured at  $P_{SAT}$

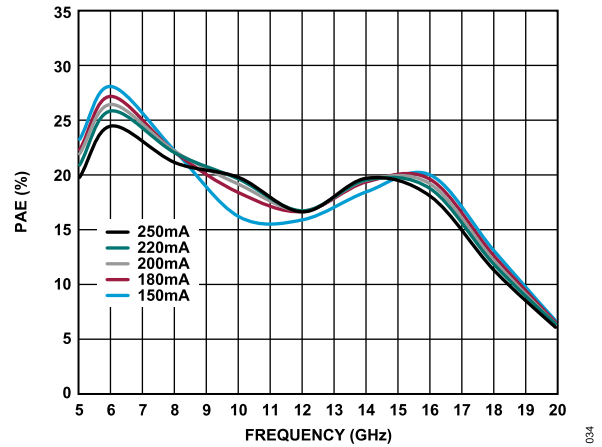


Figure 34. PAE vs. Frequency for Various  $I_{DQ\_PA}$ , Transmit State, Path = TX\_IN to ANT,  $V_{DD\_PA} = 5\text{ V}$ , Receive State Off, PAE Measured at  $P_{SAT}$

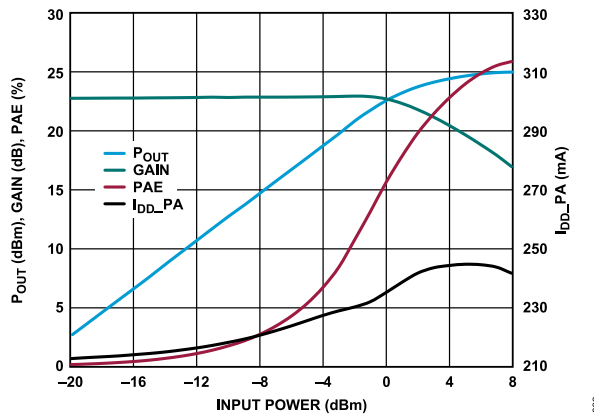


Figure 32.  $P_{OUT}$ , Gain, PAE and Power Amplifier Supply Current ( $I_{DQ\_PA}$ ) vs. Input Power, 6 GHz, Transmit State, Path = TX\_IN to ANT,  $V_{DD\_PA} = 5\text{ V}$ ,  $I_{DQ\_PA} = 220\text{ mA}$ , Receive State Off

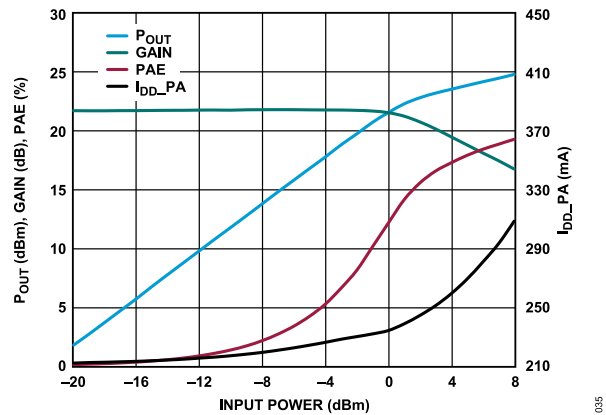


Figure 35.  $P_{OUT}$ , Gain, PAE and  $I_{DQ\_PA}$  vs. Input Power, 10 GHz, Transmit State, Path = TX\_IN to ANT,  $V_{DD\_PA} = 5\text{ V}$ ,  $I_{DQ\_PA} = 220\text{ mA}$ , Receive State Off

TYPICAL PERFORMANCE CHARACTERISTICS

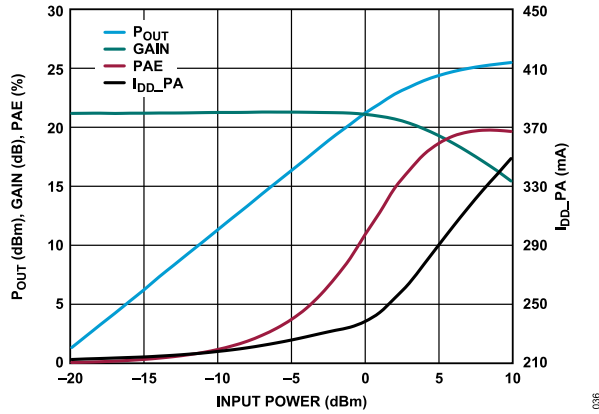


Figure 36.  $P_{OUT}$ , Gain, PAE and  $I_{DD\_PA}$  vs. Input Power, 14 GHz, Transmit State, Path = TX\_IN to ANT,  $V_{DD\_PA} = 5\text{ V}$ ,  $I_{DQ\_PA} = 220\text{ mA}$ , Receive State Off

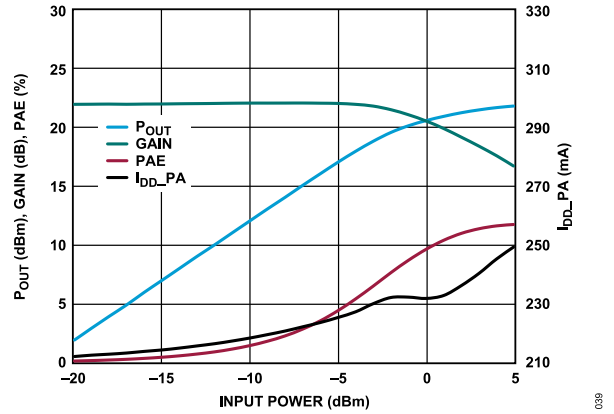


Figure 39.  $P_{OUT}$ , Gain, PAE and  $I_{DD\_PA}$  vs. Input Power, 18 GHz, Transmit State, Path = TX\_IN to ANT,  $V_{DD\_PA} = 5\text{ V}$ ,  $I_{DQ\_PA} = 220\text{ mA}$ , Receive State Off

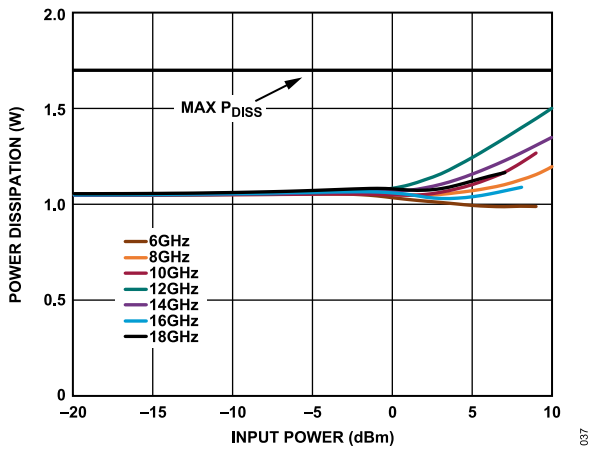


Figure 37. Power Dissipation vs. Input Power at  $T_A = 85^\circ\text{C}$ , Transmit State, Path = TX\_IN to ANT,  $V_{DD\_PA} = 5\text{ V}$ ,  $I_{DQ\_PA} = 220\text{ mA}$ , Receive State Off

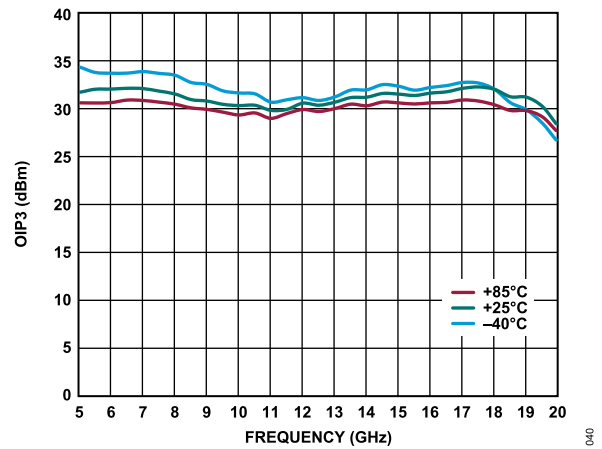


Figure 40. OIP3 vs. Frequency for Various Temperatures,  $P_{OUT}/\text{Tone} = 8\text{ dBm}$ , Transmit State, Path = TX\_IN to ANT,  $V_{DD\_PA} = 5\text{ V}$ ,  $I_{DQ\_PA} = 220\text{ mA}$ , Receive State Off

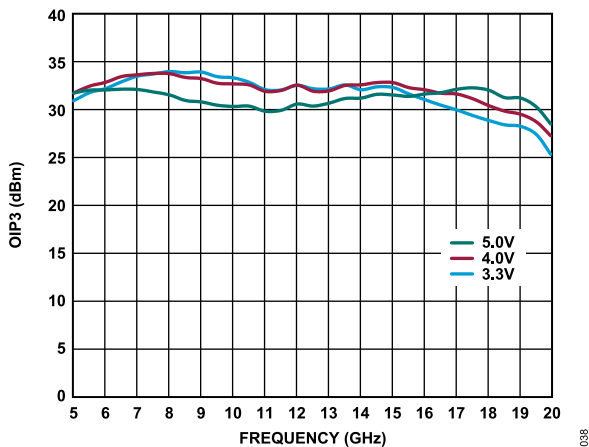


Figure 38. OIP3 vs. Frequency for Various  $V_{DD\_PA}$ ,  $P_{OUT}/\text{Tone} = 8\text{ dBm}$ , Transmit State, Path = TX\_IN to ANT,  $I_{DQ\_PA} = 220\text{ mA}$ , Receive State Off

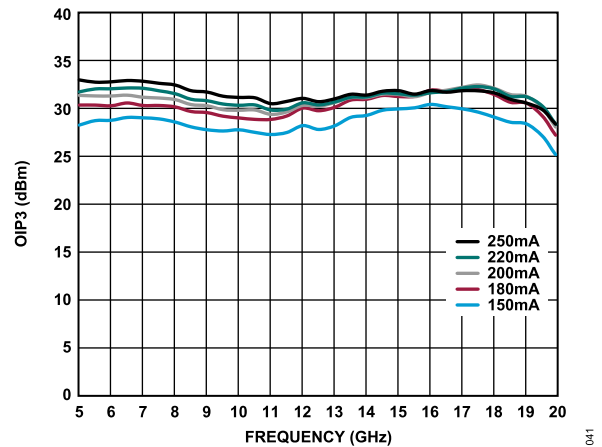


Figure 41. OIP3 vs. Frequency for Various  $I_{DQ\_PA}$ ,  $P_{OUT}/\text{Tone} = 8\text{ dBm}$ , Transmit State, Path = TX\_IN to ANT,  $V_{DD\_PA} = 5\text{ V}$ , Receive State Off

TYPICAL PERFORMANCE CHARACTERISTICS

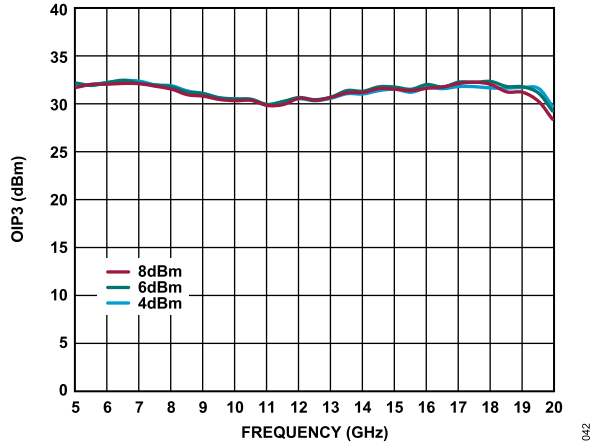


Figure 42. OIP3 vs. Frequency for Various  $P_{OUT}/Tone$ , Transmit State, Path = TX\_IN to ANT,  $V_{DD\_PA} = 5\text{ V}$ ,  $I_{DQ\_PA} = 220\text{ mA}$ , Receive State Off

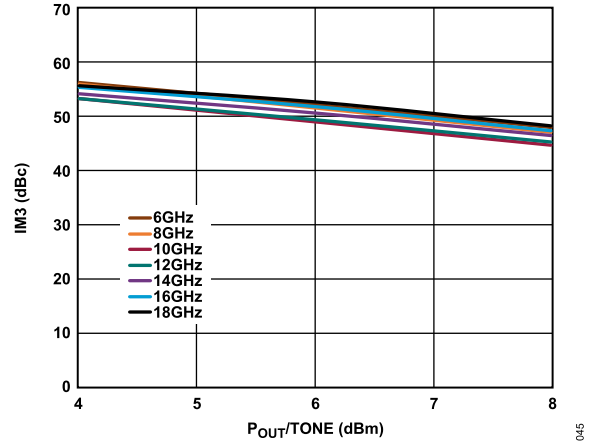


Figure 45. Third-Order Intermodulation Distortion Relative to Carrier (IM3) vs.  $P_{OUT}/Tone$ , Transmit State, Path = TX\_IN to ANT,  $V_{DD\_PA} = 5\text{ V}$ ,  $I_{DQ\_PA} = 220\text{ mA}$ , Receive State Off

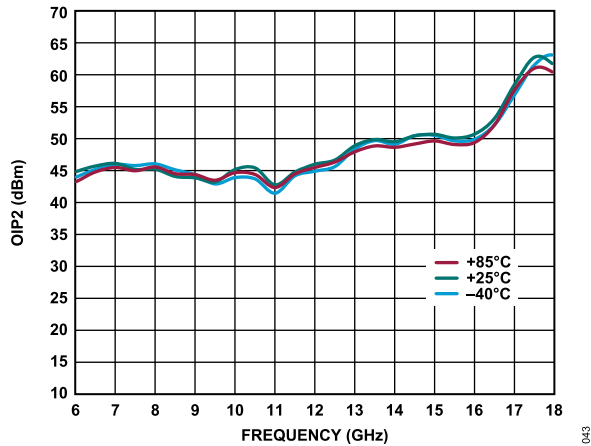


Figure 43. Output Second-Order Intercept (OIP2) vs. Frequency for Various Temperatures,  $P_{OUT}/Tone = 8\text{ dBm}$ , Transmit State, Path = TX\_IN to ANT,  $V_{DD\_PA} = 5\text{ V}$ ,  $I_{DQ\_PA} = 220\text{ mA}$ , Receive State Off

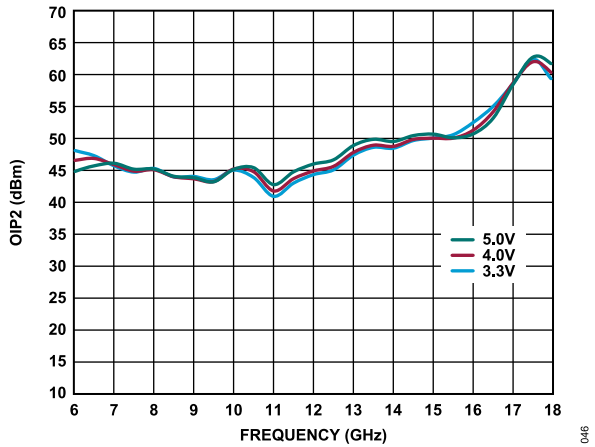


Figure 46. OIP2 vs. Frequency for Various  $V_{DD\_PA}$ ,  $P_{OUT}/Tone = 8\text{ dBm}$ , Transmit State, Path = TX\_IN to ANT,  $I_{DQ\_PA} = 220\text{ mA}$ , Receive State Off

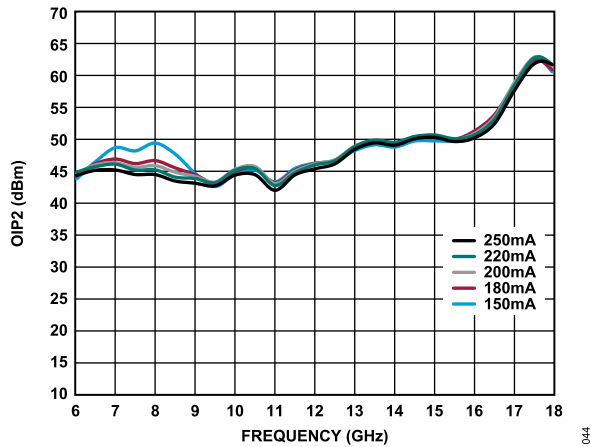


Figure 44. OIP2 vs. Frequency for Various  $I_{DQ\_PA}$ ,  $P_{OUT}/Tone = 8\text{ dBm}$ , Transmit State, Path = TX\_IN to ANT,  $V_{DD\_PA} = 5\text{ V}$ , Receive State Off

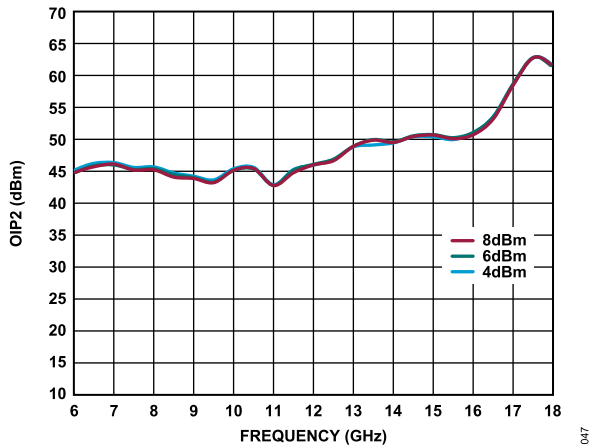


Figure 47. OIP2 vs. Frequency for Various  $P_{OUT}/Tone$ , Transmit State, Path = TX\_IN to ANT,  $V_{DD\_PA} = 5\text{ V}$ ,  $I_{DQ\_PA} = 220\text{ mA}$ , Receive State Off

TYPICAL PERFORMANCE CHARACTERISTICS

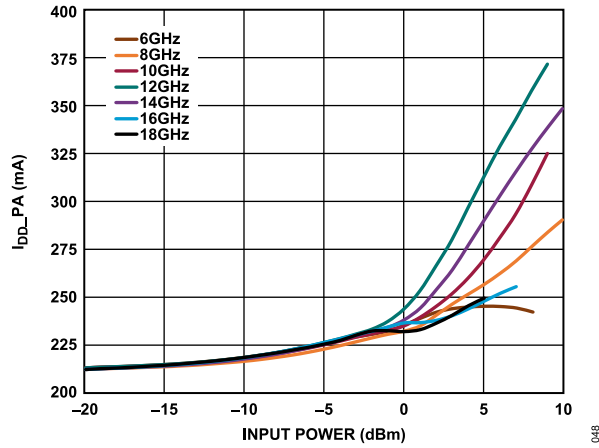


Figure 48.  $I_{DD\_PA}$  vs. Input Power for Various Frequencies, Transmit State, Path = TX\_IN to ANT, VDD\_PA = 5 V,  $I_{DQ\_PA}$  = 220 mA, Receive State Off

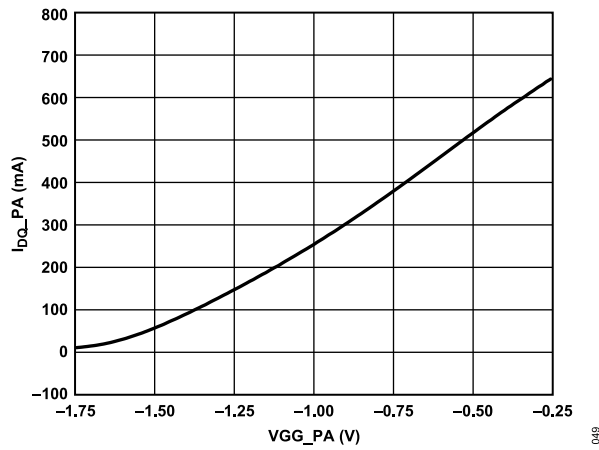


Figure 49.  $I_{DQ\_PA}$  vs. VGG\_PA, VDD\_PA = 5 V, Transmit State, Path = TX\_IN to ANT, VDD\_PA = 5 V, Receive State Off

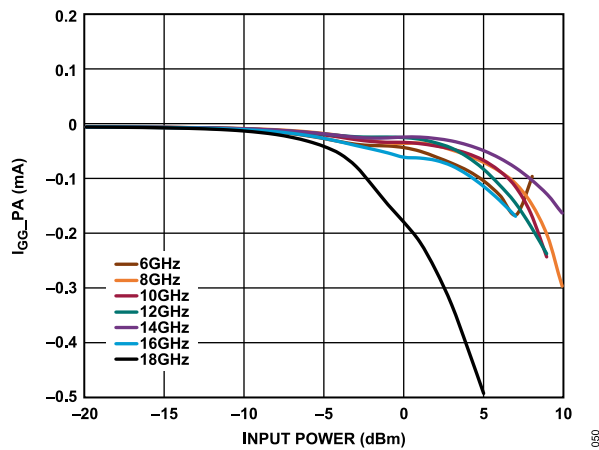


Figure 50. Power Amplifier Gate Current ( $I_{GG\_PA}$ ) vs. Input Power for Various Frequencies, Transmit State, Path = TX\_IN to ANT, VDD\_PA = 5 V,  $I_{DQ\_PA}$  = 220 mA, Receive State Off

TYPICAL PERFORMANCE CHARACTERISTICS

RECEIVE STATE

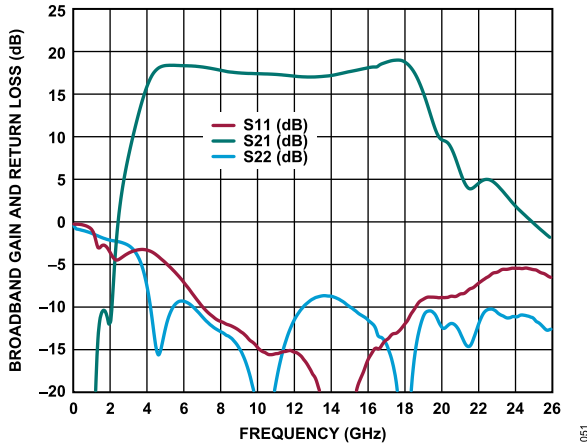


Figure 51. Broadband Gain and Return Loss vs. Frequency, 10 MHz to 26 GHz, Receive State, Path = ANT to RX\_OUT, Self Biased Mode, VDD\_LNA = 3.3 V, VGG\_LNA = 0 V, Transmit State Off

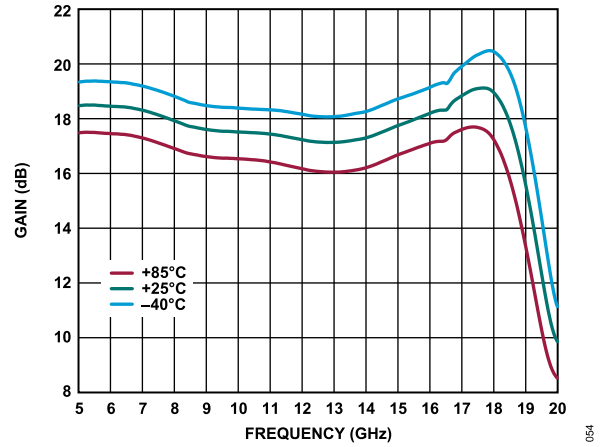


Figure 54. Gain vs. Frequency for Various Temperatures, Receive State, Path = ANT to RX\_OUT, Self Biased Mode, VDD\_LNA = 3.3 V, VGG\_LNA = 0 V, Transmit State Off

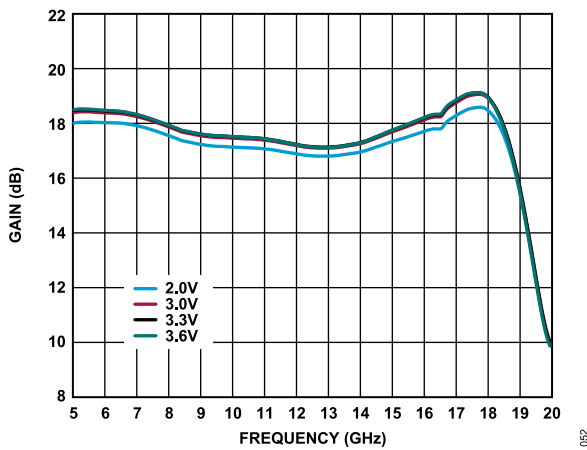


Figure 52. Gain vs. Frequency for Various VDD\_LNA, Receive State, Path = ANT to RX\_OUT, Self Biased Mode, VGG\_LNA = 0 V, Transmit State Off

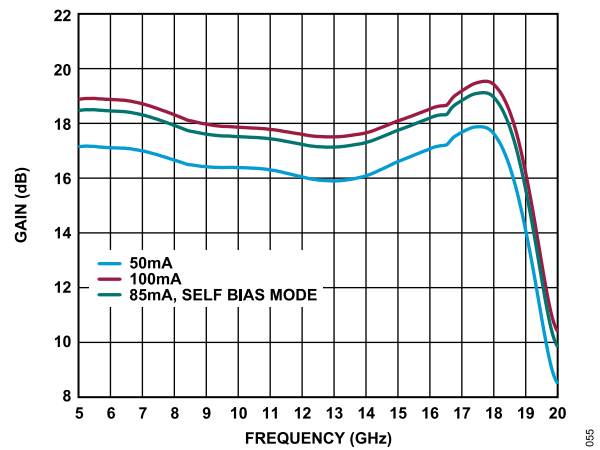


Figure 55. Gain vs. Frequency for Various IDQ\_LNA, Receive State, Path = ANT to RX\_OUT, Self Biased Mode, VDD\_LNA = 3.3 V, Controlled VGG\_LNA, Transmit State Off

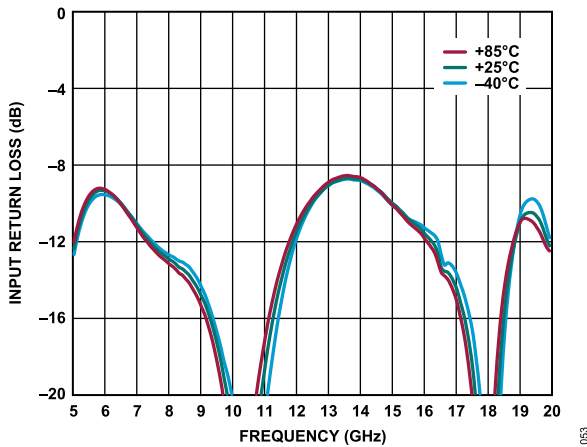


Figure 53. Input Return Loss vs. Frequency for Various Temperatures, Receive State, Path = ANT to RX\_OUT, Self Biased Mode, VDD\_LNA = 3.3 V, VGG\_LNA = 0 V, Transmit State Off



TYPICAL PERFORMANCE CHARACTERISTICS

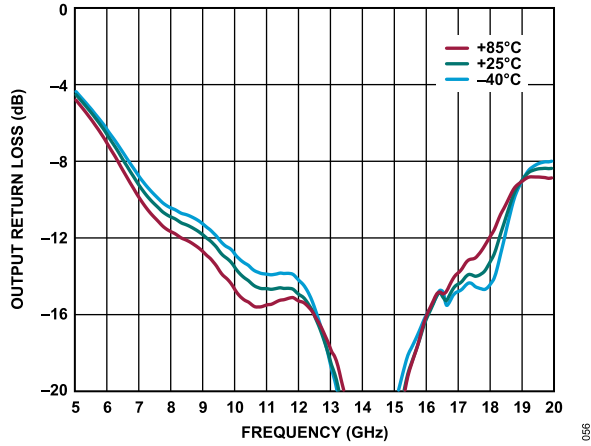


Figure 56. Output Return Loss vs. Frequency for Various Temperatures, Receive State, Path = ANT to RX\_OUT, Self Biased Mode, VDD\_LNA = 3.3 V, VGG\_LNA = 0 V, Transmit State Off

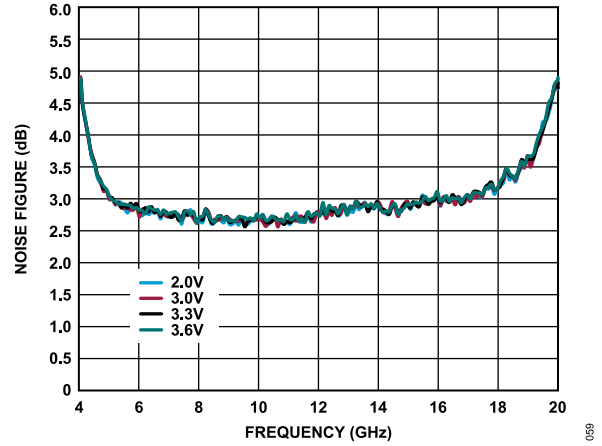


Figure 59. Noise Figure vs. Frequency for Various VDD\_LNA, Receive State, Path = ANT to RX\_OUT, Self Biased Mode, VGG\_LNA = 0 V, Transmit State Off

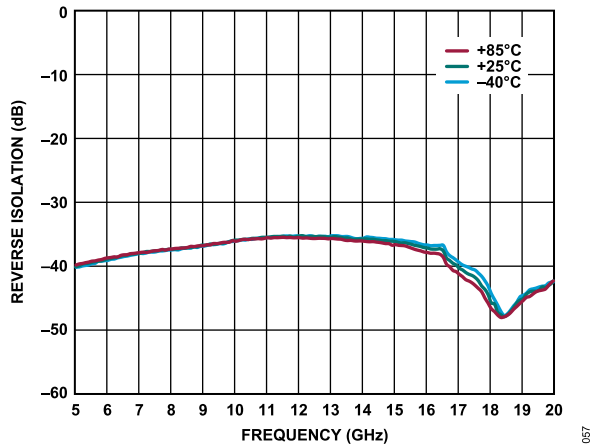


Figure 57. Reverse Isolation vs. Frequency for Various Temperatures, Receive State, Path = ANT to RX\_OUT, Self Biased Mode, VDD\_LNA = 3.3 V, VGG\_LNA = 0 V, Transmit State Off

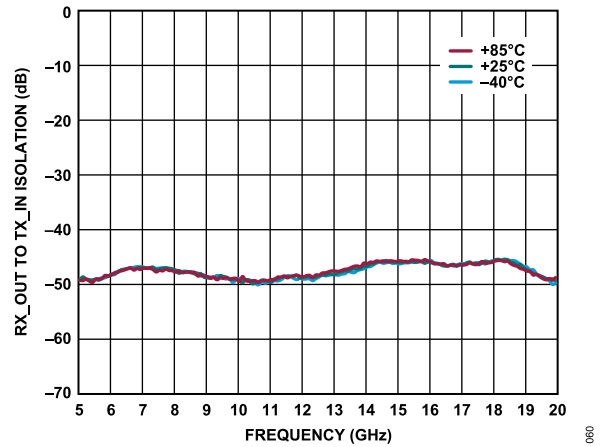


Figure 60. RX\_OUT to TX\_IN Isolation vs. Frequency for Various Temperatures, Receive State, Path = ANT to RX\_OUT, Self Biased Mode, VDD\_LNA = 3.3 V, VGG\_LNA = 0 V, Transmit State Off

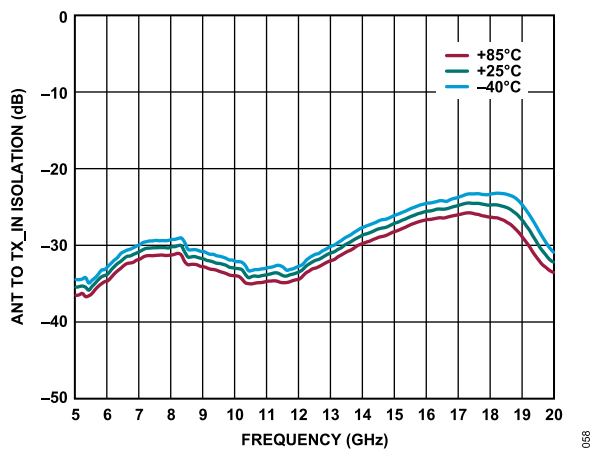


Figure 58. ANT to TX\_IN Isolation vs. Frequency for Various Temperatures, Receive State, Path = ANT to RX\_OUT, Self Biased Mode, VDD\_LNA = 3.3 V, VGG\_LNA = 0 V, Transmit State Off

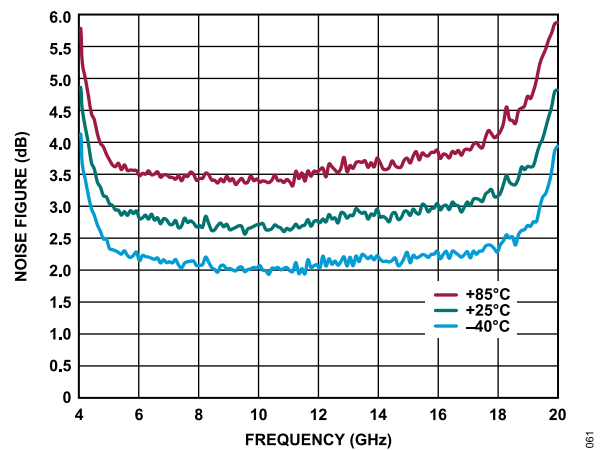


Figure 61. Noise Figure vs. Frequency for Various Temperatures, Receive State, Path = ANT to RX\_OUT, Self Biased Mode, VDD\_LNA = 3.3 V, VGG\_LNA = 0 V, Transmit State Off

TYPICAL PERFORMANCE CHARACTERISTICS

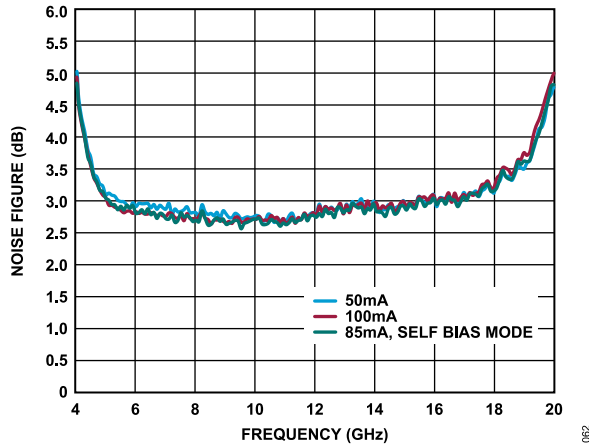


Figure 62. Noise Figure vs. Frequency for Various  $I_{DQ\_LNA}$ , Receive State, Path = ANT to RX\_OUT, Self Biased Mode,  $V_{DD\_LNA} = 3.3\text{ V}$ , Controlled VGG\_LNA, Transmit State Off

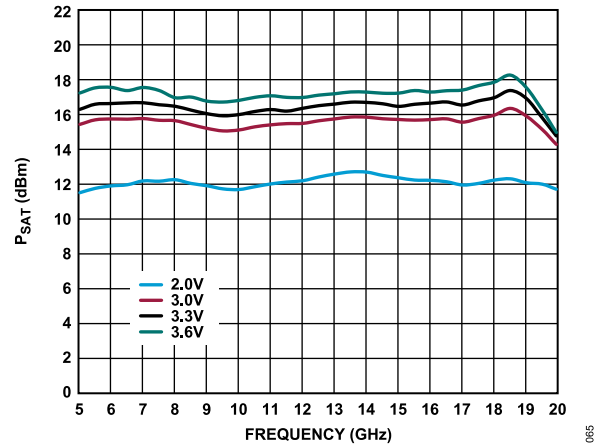


Figure 65.  $P_{SAT}$  vs. Frequency for Various  $V_{DD\_LNA}$ , Receive State, Path = ANT to RX\_OUT, Self Biased Mode,  $V_{GG\_LNA} = 0\text{ V}$ , Transmit State Off

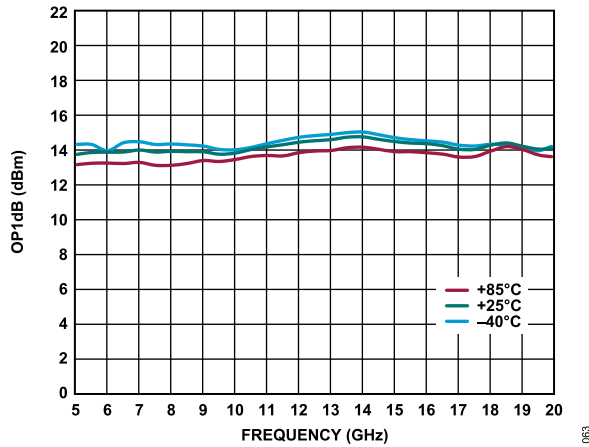


Figure 63. OP1dB vs. Frequency for Various Temperatures, Receive State, Path = ANT to RX\_OUT, Self Biased Mode,  $V_{DD\_LNA} = 3.3\text{ V}$ ,  $V_{GG\_LNA} = 0\text{ V}$ , Transmit State Off

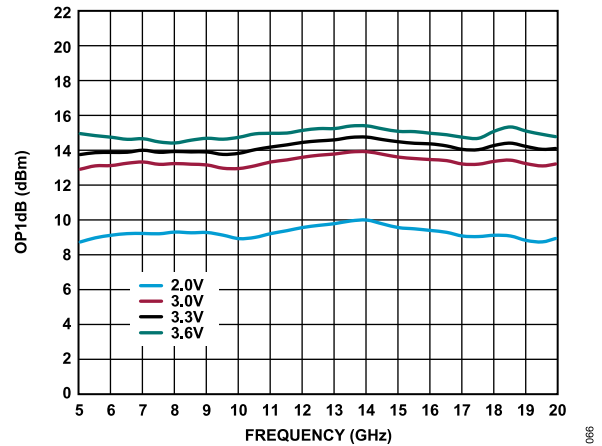


Figure 66. OP1dB vs. Frequency for Various  $V_{DD\_LNA}$ , Receive State, Path = ANT to RX\_OUT, Self Biased Mode,  $V_{GG\_LNA} = 0\text{ V}$ , Transmit State Off

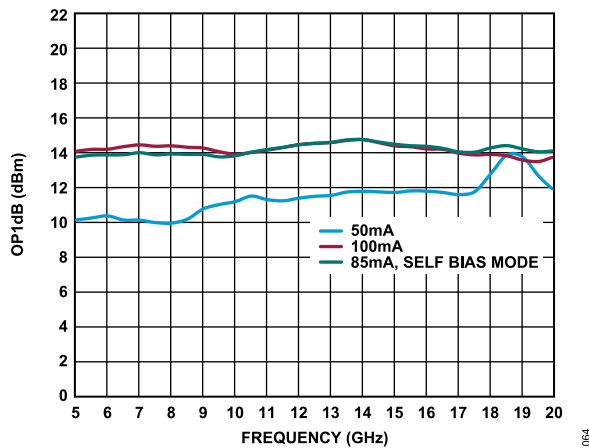


Figure 64. OP1dB vs. Frequency for Various  $I_{DQ\_LNA}$ , Receive State, Path = ANT to RX\_OUT, Self Biased Mode,  $V_{DD\_LNA} = 3.3\text{ V}$ , Controlled VGG\_LNA, Transmit State Off

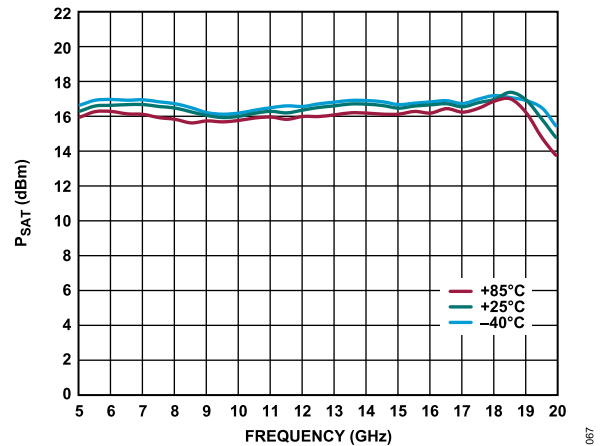


Figure 67.  $P_{SAT}$  vs. Frequency for Various Temperatures, Receive State, Path = ANT to RX\_OUT, Self Biased Mode,  $V_{DD\_LNA} = 3.3\text{ V}$ ,  $V_{GG\_LNA} = 0\text{ V}$ , Transmit State = Off

TYPICAL PERFORMANCE CHARACTERISTICS

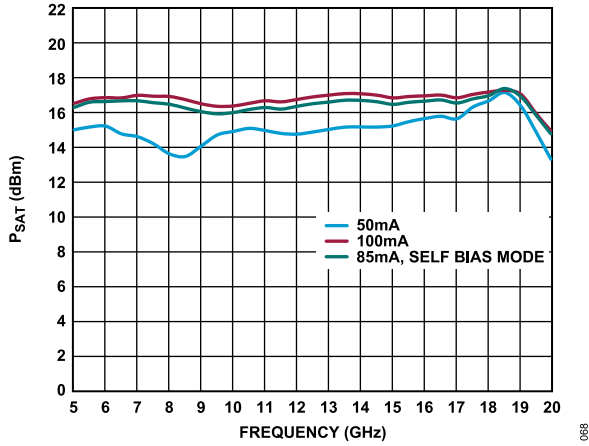


Figure 68.  $P_{SAT}$  vs. Frequency for Various  $I_{DD\_LNA}$ , Receive State, Path = ANT to RX\_OUT, Self Biased Mode,  $V_{DD\_LNA} = 3.3\text{ V}$ , Controlled  $V_{GG\_LNA}$ , Transmit State Off

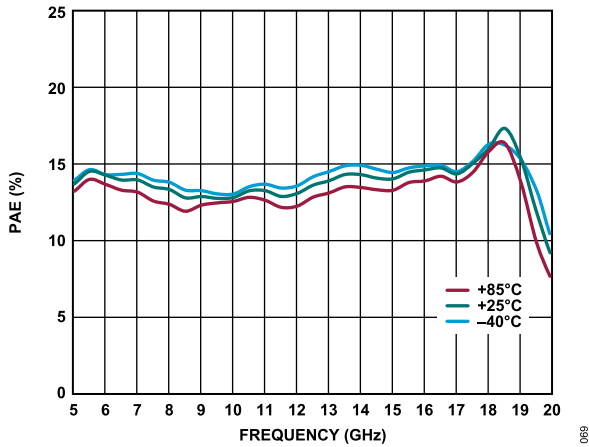


Figure 69. PAE vs. Frequency for Various Temperatures, Receive State, Path = ANT to RX\_OUT, Self Biased Mode,  $V_{DD\_LNA} = 3.3\text{ V}$ ,  $V_{GG\_LNA} = 0\text{ V}$ , Transmit State Off, PAE Measured at  $P_{SAT}$

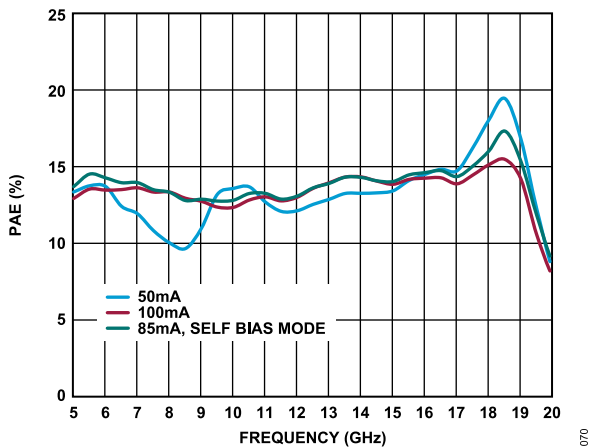


Figure 70. PAE vs. Frequency for Various  $I_{DD\_LNA}$ , Receive State, Path = ANT to RX\_OUT, Self Biased Mode,  $V_{DD\_LNA} = 3.3\text{ V}$ , Controlled  $V_{GG\_LNA}$ , Transmit State Off, PAE Measured at  $P_{SAT}$

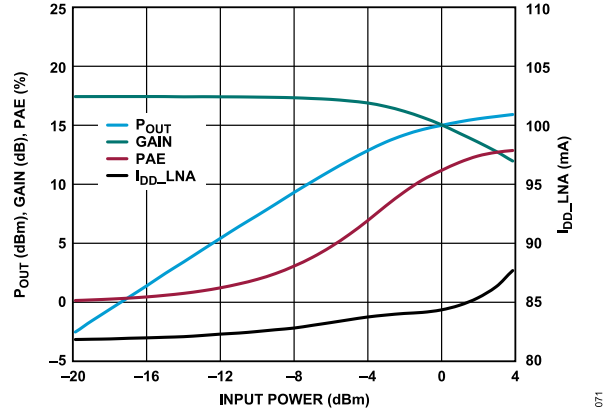


Figure 71.  $P_{OUT}$ , Gain, PAE and  $I_{DD\_LNA}$  vs. Input Power, 10 GHz, Receive State, Path = ANT to RX\_OUT, Self Biased Mode,  $V_{DD\_LNA} = 3.3\text{ V}$ ,  $V_{GG\_LNA} = 0\text{ V}$ , Transmit State Off

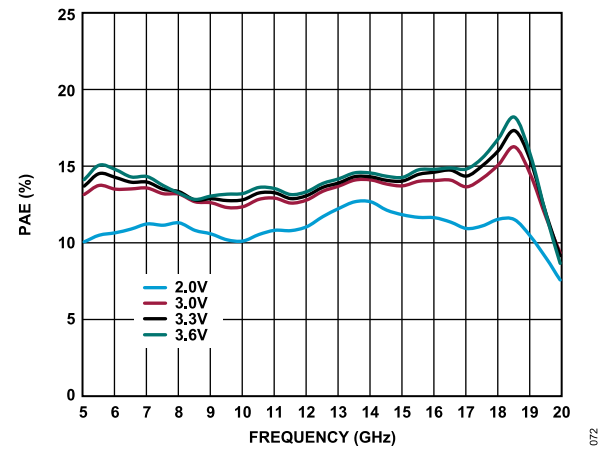


Figure 72. PAE vs. Frequency for Various  $V_{DD\_LNA}$ , Receive State, Path = ANT to RX\_OUT, Self Biased Mode,  $V_{GG\_LNA} = 0\text{ V}$ , Transmit State Off, PAE Measured at  $P_{SAT}$

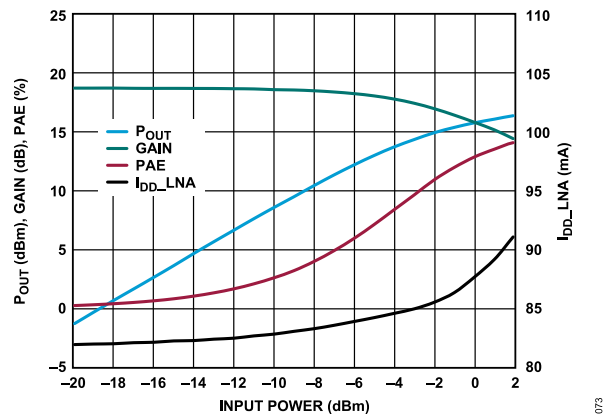


Figure 73.  $P_{OUT}$ , Gain, PAE and  $I_{DD\_LNA}$  vs. Input Power, 6 GHz, Receive State, Path = ANT to RX\_OUT, Self Biased Mode,  $V_{DD\_LNA} = 3.3\text{ V}$ ,  $V_{GG\_LNA} = 0\text{ V}$ , Transmit State Off

TYPICAL PERFORMANCE CHARACTERISTICS

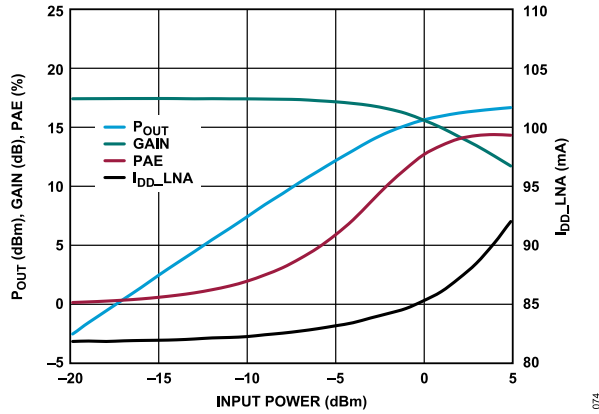


Figure 74.  $P_{OUT}$ , Gain, PAE and  $I_{DD\_LNA}$  vs. Input Power, 14 GHz, Receive State, Path = ANT to RX\_OUT, Self Biased Mode,  $V_{DD\_LNA} = 3.3\text{ V}$ ,  $V_{GG\_LNA} = 0\text{ V}$ , Transmit State Off

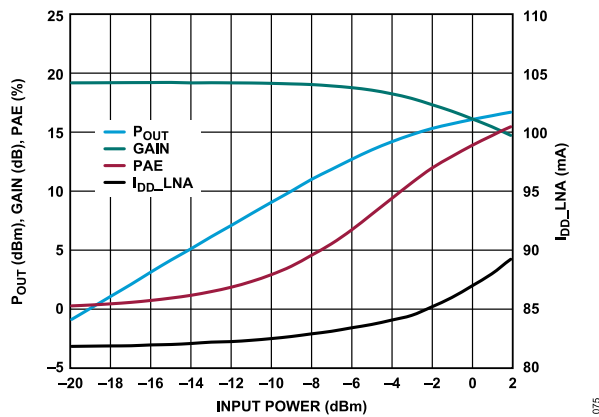


Figure 75.  $P_{OUT}$ , Gain, PAE and  $I_{DD\_LNA}$  vs. Input Power, 18 GHz, Receive State, Path = ANT to RX\_OUT, Self Biased Mode,  $V_{DD\_LNA} = 3.3\text{ V}$ ,  $V_{GG\_LNA} = 0\text{ V}$ , Transmit State Off

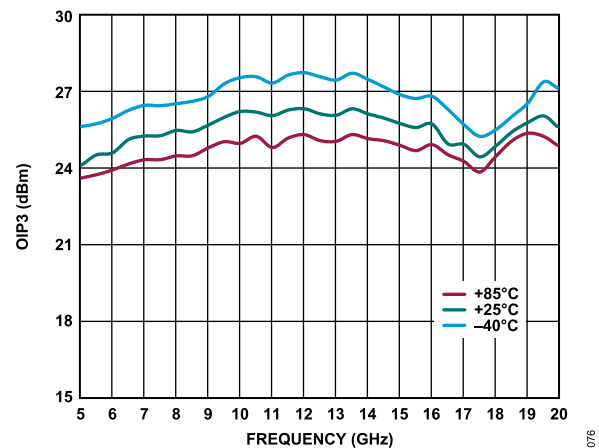


Figure 76. OIP3 vs. Frequency for Various Temperatures,  $P_{OUT}/\text{Tone} = 0\text{ dBm}$ , Receive State, Path = ANT to RX\_OUT, Self Biased Mode,  $V_{DD\_LNA} = 3.3\text{ V}$ ,  $V_{GG\_LNA} = 0\text{ V}$ , Transmit State Off

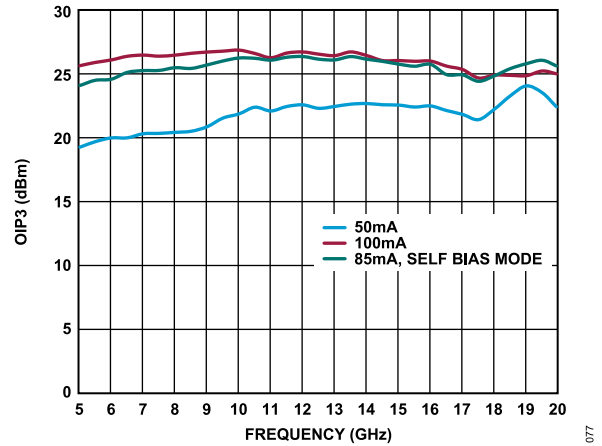


Figure 77. OIP3 vs. Frequency for Various  $I_{DD\_LNA}$ ,  $P_{OUT}/\text{Tone} = 0\text{ dBm}$ , Receive State, Path = ANT to RX\_OUT, Self Biased Mode,  $V_{DD\_LNA} = 3.3\text{ V}$ , Controlled  $V_{GG\_LNA}$ , Transmit State Off

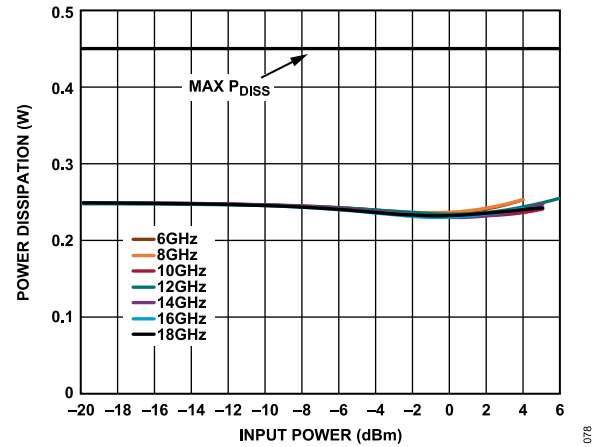


Figure 78. Power Dissipation vs. Input Power at  $T_A = 85^\circ\text{C}$ , Receive State, Path = ANT to RX\_OUT, Self Biased Mode,  $V_{DD\_LNA} = 3.3\text{ V}$ ,  $V_{GG\_LNA} = 0\text{ V}$ , Transmit State Off

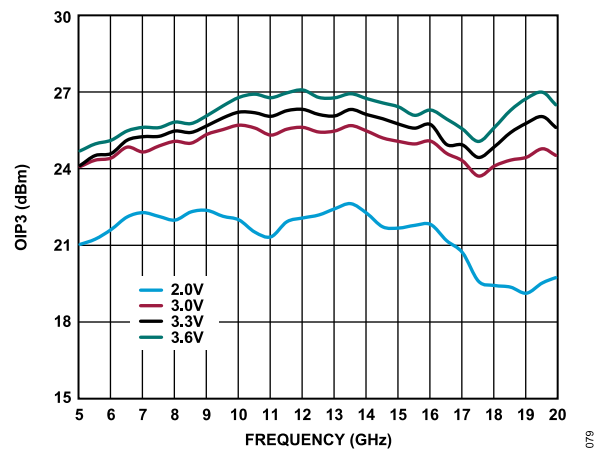


Figure 79. OIP3 vs. Frequency for Various  $V_{DD\_LNA}$ ,  $P_{OUT}/\text{Tone} = 0\text{ dBm}$ , Receive State, Path = ANT to RX\_OUT, Self Biased Mode,  $V_{GG\_LNA} = 0\text{ V}$ , Transmit State Off

TYPICAL PERFORMANCE CHARACTERISTICS

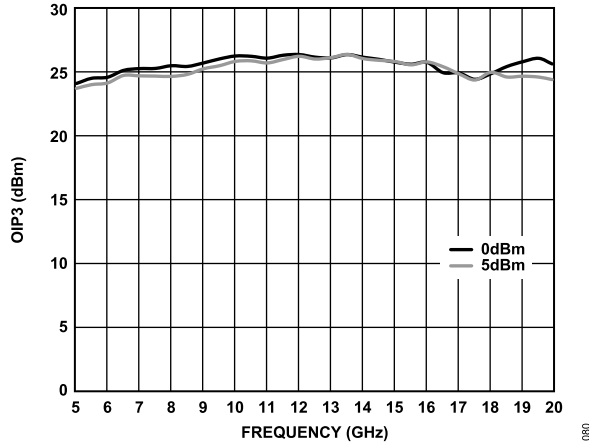


Figure 80. OIP3 vs. Frequency for Various  $P_{OUT}/Tone$ , Receive State, Path = ANT to RX\_OUT, Self Biased Mode,  $V_{DD\_LNA} = 3.3\text{ V}$ ,  $V_{GG\_LNA} = 0\text{ V}$ , Transmit State Off

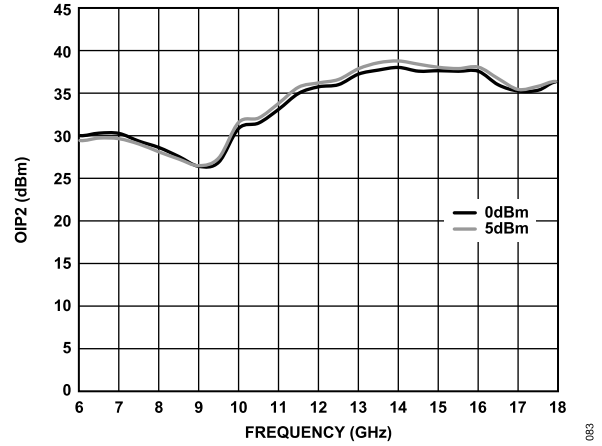


Figure 83. OIP2 vs. Frequency for Various  $P_{OUT}/Tone$ , Receive State, Path = ANT to RX\_OUT, Self Biased Mode,  $V_{DD\_LNA} = 3.3\text{ V}$ ,  $V_{GG\_LNA} = 0\text{ V}$ , Transmit State Off

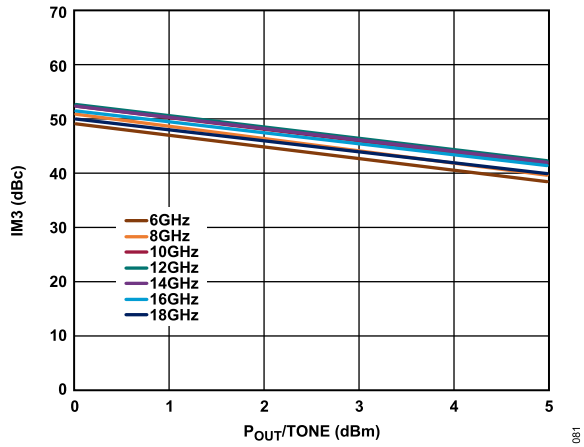


Figure 81. IM3 vs.  $P_{OUT}/Tone$ , Receive State, Path = ANT to RX\_OUT, Self Biased Mode,  $V_{DD\_LNA} = 3.3\text{ V}$ ,  $V_{GG\_LNA} = 0\text{ V}$ , Transmit State Off

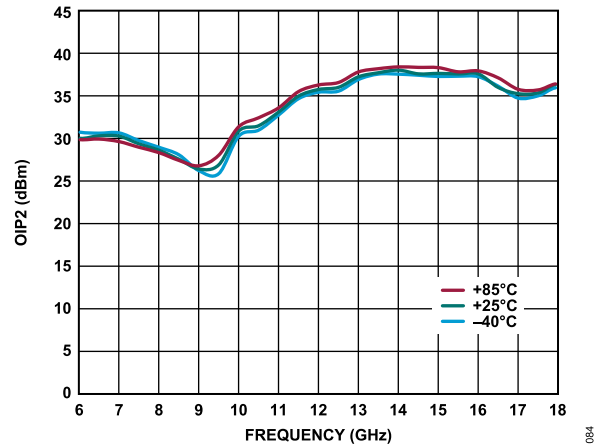


Figure 84. OIP2 vs. Frequency for Various Temperatures,  $P_{OUT}/Tone = 0\text{ dBm}$ , Receive State, Path = ANT to RX\_OUT, Self Biased Mode,  $V_{DD\_LNA} = 3.3\text{ V}$ ,  $V_{GG\_LNA} = 0\text{ V}$ , Transmit State Off

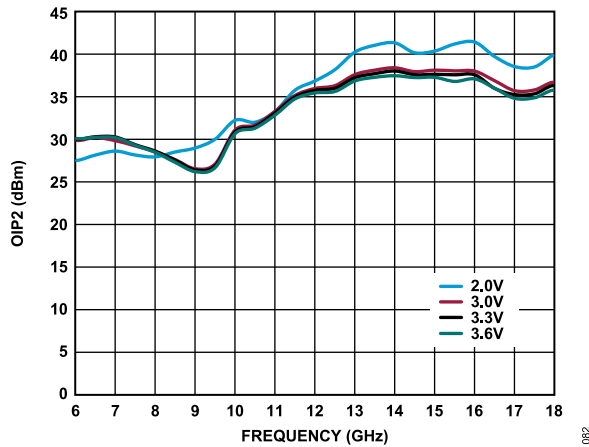


Figure 82. OIP2 vs. Frequency for Various  $V_{DD\_LNA}$ ,  $P_{OUT}/Tone = 0\text{ dBm}$ , Receive State, Path = ANT to RX\_OUT, Self Biased Mode,  $V_{GG\_LNA} = 0\text{ V}$ , Transmit State Off

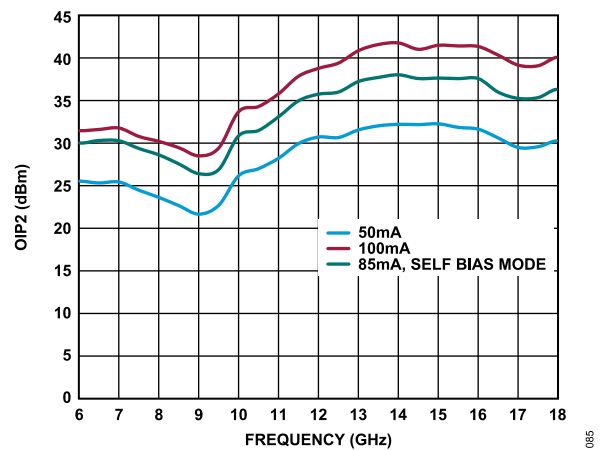


Figure 85. OIP2 vs. Frequency for Various  $I_{DQ\_LNA}$ ,  $P_{OUT}/Tone = 0\text{ dBm}$ , Receive State, Path = ANT to RX\_OUT, Self Biased Mode,  $V_{DD\_LNA} = 3.3\text{ V}$ , Controlled  $V_{GG\_LNA}$ , Transmit State Off

TYPICAL PERFORMANCE CHARACTERISTICS

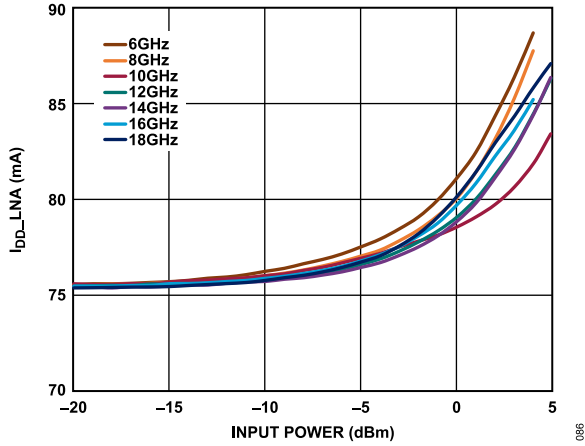


Figure 86.  $I_{DD\_LNA}$  vs. Input Power for Various Frequencies, Receive State, Path = ANT to RX\_OUT, Self Biased Mode,  $V_{DD\_LNA} = 3.3$  V,  $V_{GG\_LNA} = 0$  V, Transmit State Off

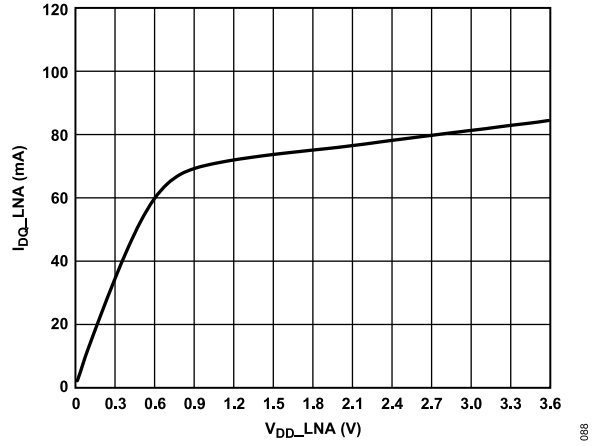


Figure 88.  $I_{DQ\_LNA}$  vs.  $V_{DD\_LNA}$ , Self Biased Mode,  $V_{GG\_LNA} = 0$  V, Receive State, Path = ANT to RX\_OUT, Transmit State Off

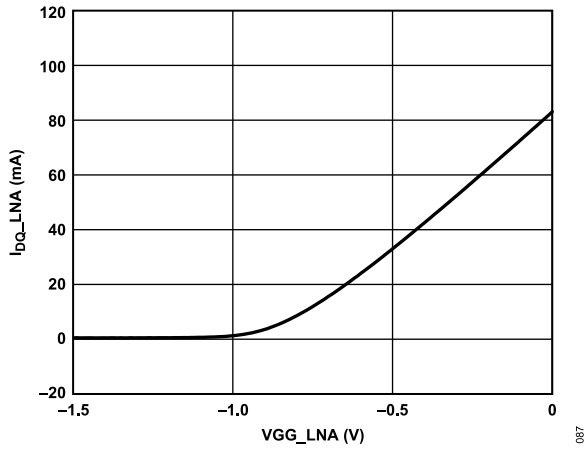


Figure 87.  $I_{DQ\_LNA}$  vs.  $V_{GG\_LNA}$ ,  $V_{DD\_LNA} = 3.3$  V, Controlled  $V_{GG\_LNA}$ , Receive State, Path = ANT to RX\_OUT, Transmit State Off

## THEORY OF OPERATION

The ADTR1107 is a multichip transmit/receive module that consists of an LNA, a medium power amplifier, and a silicon SPDT reflective switch. The ANT antenna port is dc-coupled to 0 V and no dc block is required at this port when the RF line potential is equal to 0 V. The switch has an integrated driver to perform logic functions internally and provides a simplified complementary metal-oxide semiconductor (CMOS)/low voltage transistor to transistor logic (LVTTTL)-compatible control interface. The driver features a single digital control input pin, CTRL\_SW. The logic level applied to CTRL\_SW determines whether the ADTR1107 is in transmit state or receive state (see [Table 8](#)).

The receive path contains a self biased LNA with optional bias control using the VGG\_LNA pin for bias adjustment. For self biased

operation, the VGG\_LNA pin is set to 0 V or connected to ground. The receive path output (RX\_OUT) is dc-coupled to ground through an 8 k $\Omega$  resistor. No dc block is required at this port when the RF line potential is equal to 0 V.

The transmit path contains a power amplifier. The bias current is set using VGG\_PA. The transmit path input (TX\_IN) is dc-coupled to ground through a 2.5 k $\Omega$  resistor. No dc block is required at this port when the RF line potential is equal to 0 V. A directional coupler is incorporated into the ADTR1107 to allow for monitoring of the transmit power level.

## APPLICATIONS INFORMATION

The basic connections for operating the ADTR1107 are shown in [Figure 89](#). The power amplifier on the transmit path is biased with +5 V on the VDD\_PA pin and a voltage from -1.75 V to -0.25 V is applied to the VGG\_PA pin to achieve 220 mA quiescent current.

The LNA on the receive path operates as either self biased or external biased mode. For self biased mode, apply 3.3 V to the VDD\_LNA pin and leave the VGG\_LNA pin supplied with 0 V or connected to ground. For external biased mode, apply +3.3 V to the VDD\_LNA pin and adjust the VGG\_LNA pin with a voltage range of -1.5 V to 0 V to achieve the desired  $I_{DQ\_PA}$ .

The SPDT switch is biased with +3.3 V on the VDD\_SW pin and -3.3 V on the VSS\_SW pin. The CTRL\_SW pin sets the path state shown in [Table 8](#). The high logic state is set at 3.3 V, and the low logic state is set at 0 V.

### RECOMMENDED BIAS SEQUENCING

The recommended bias sequence during transmit state power-up is as follows:

1. Connect all GND pins to ground.
2. Set the VDD\_SW pin to 3.3 V.
3. Set the VSS\_SW pin to -3.3 V.
4. Set the CTRL\_SW pin to 0 V.
5. Set the VGG\_LNA pin to 0 V.
6. Set the VDD\_LNA pin to 0 V.
7. Set the VGG\_PA pin to -1.75 V.
8. Set the VDD\_PA pin to 5 V.
9. Increase the VGG\_PA voltage to achieve the desired  $I_{DQ\_PA}$ .
10. Apply the RF signal to the TX\_IN pin.

The recommended transmit state bias sequence during power-down is as follows:

1. Turn off the RF signal.
2. Decrease the VGG\_PA voltage to -1.75 V.
3. Set the VDD\_PA pin to 0 V.

4. Set the VSS\_SW pin to 0 V.
5. Set the VDD\_SW pin to 0 V.

The recommended bias sequence during receive state power-up is as follows:

1. Connect all GND pins to ground.
2. Set the VDD\_SW pin to 3.3 V.
3. Set the VSS\_SW pin to -3.3 V.
4. Set the CTRL\_SW pin to 3.3 V.
5. Set the VGG\_PA pin to -1.75 V.
6. Set the VDD\_PA pin to 0 V.
7. Set the VGG\_LNA pin to 0 V.
8. Set the VDD\_LNA pin to 3.3 V.
9. Apply the RF signal to the ANT pin.

The recommended receive state bias sequence during power-down is as follows:

1. Turn off the RF signal.
2. Set the VDD\_LNA pin to 0 V.
3. Set the CTRL\_SW pin to 0 V.
4. Set the VSS\_SW pin to 0 V.
5. Set the VDD\_SW pin to 0 V.

All measurements and data shown in this data sheet were taken using the typical application circuit (see [Figure 89](#)) and biased per the conditions in this section, unless otherwise noted. The bias conditions described in this section are the operating points recommended to optimize the overall device performance. Operation using other bias conditions can result in performance that differs from what is shown in the [Typical Performance Characteristics](#) section. To obtain optimal performance while not damaging the device, follow the recommended biasing sequences described in this section and adhere to the values shown in the [Absolute Maximum Ratings](#) section.



APPLICATIONS INFORMATION

TYPICAL APPLICATION CIRCUIT

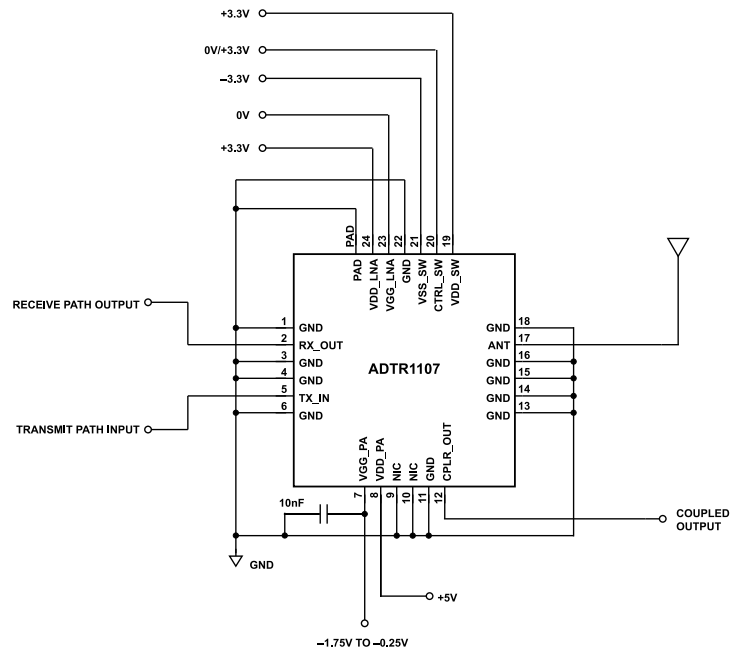


Figure 89. Typical Application Circuit

**INTERFACING THE ADTR1107 TO THE ADAR1000 X BAND AND KU BAND BEAMFORMER**

The ADTR1107 can be interfaced to the ADAR1000 X band and Ku band quad beamformer IC, as shown in Figure 91. Note that only a single channel of the ADAR1000 is shown in Figure 91 and additional components have been omitted for clarity. The ADAR1000 provides multiple bias voltages and control signals, resulting in a glueless interface and no need for any additional control signals to the ADTR1107. The gate voltage for the ADTR1107 power amplifier (VGG\_PA) is provided by the ADAR1000 PA\_BIAS3 pin. One of four independent negative gate voltages is needed for power amplifier gate biasing. Each voltage is set by an 8-bit digital-to-analog converter (DAC) with an output voltage range of 0 V to -4.8 V. The typical gate voltage required to bias the ADTR1107 power amplifier is -1.1 V (see Figure 49). This voltage can be asserted by the ADAR1000 TR input pin (rising edge enables the power amplifier) or by a serial peripheral interface (SPI) write. Asserting the ADAR1000 TR pin switches the polarity of the ADAR1000 TR\_SW\_NEG pin and TR\_SW\_POS pin. The TR\_SW\_POS pin can drive the gates of up to four switches and can be used to control the ADTR1107 SPDT switch.

While the ADTR1107 LNA gate voltage is self biased (the VGG\_LNA pin is connected to 0 V or grounded), the voltage can also be controlled from the ADAR1000. In this case, there is a single LNA\_BIAS voltage (0 V to -4.8 V) controlled by an 8-bit DAC that can be used to bias four ADTR1107 devices connected to each ADAR1000.

The ADTR1107 CPLR\_OUT coupler output can be tied back to one of the four ADAR1000 RF detector inputs (DET1 to DET4). These

diode based RF detectors have an input range of -20 dBm to +10 dBm. The coupling factor of the ADTR1107 directional coupler ranges from 28 dB at 6 GHz to 18 dB at 18 GHz. At 12 GHz, with a coupling factor of 22 dB and a maximum power amplifier output of 26 dBm, the coupled output power is a maximum of 4 dBm. If the coupler output is connected directly to the detector input, this connection provides a detection range of 24 dB. Figure 90 shows the relationship between the ADTR1107 output power and the ADC code of the ADAR1000 detector at 12 GHz. In this case, the ADTR1107 output power is swept to a maximum level of approximately 22 dBm.

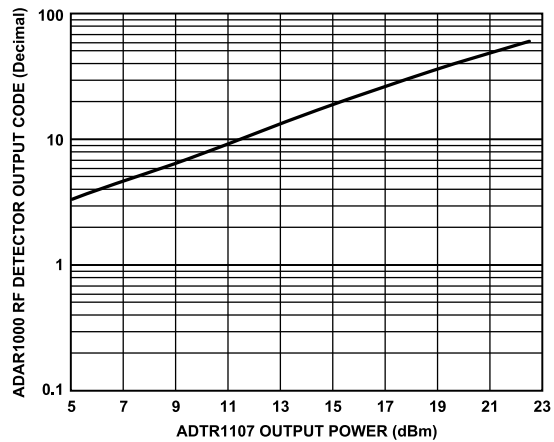


Figure 90. ADAR1000 RF Detector Output Code vs. ADTR1107 Output Power at 12 GHz

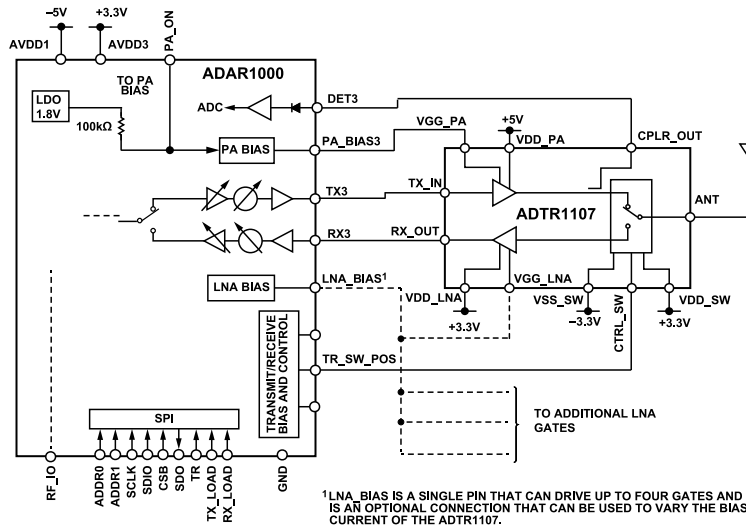


Figure 91. Interfacing the ADTR1107 to the ADAR1000 X and Ku Band Beamformer, One Channel Shown

OUTLINE DIMENSIONS

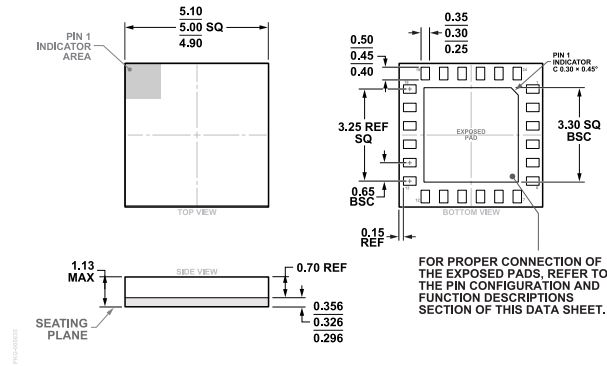


Figure 92. 24-Terminal Land Grid Array [LGA] (CC-24-8)  
Dimensions shown in millimeters

Updated: September 30, 2022

ORDERING GUIDE

Model <sup>1</sup>	Temperature Range	Package Description	Packing Quantity	Package Option
ADTR1107ACCZ	-40°C to +85°C	24-Lead LGA (5mm x 5mm x 1.13mm w/ EP)	Reel, 750	CC-24-8
ADTR1107ACCZ-R7	-40°C to +85°C	24-Lead LGA (5mm x 5mm x 1.13mm w/ EP)	Reel, 750	CC-24-8

<sup>1</sup> Z = RoHS Compliant Part.

EVALUATION BOARDS

Model <sup>1</sup>	Description
ADTR1107-EVAL	Evaluation Board

<sup>1</sup> Z = RoHS Compliant Part.